ORKUSTOFNUN
NATIONAL ENERGY AUTHORITY
HYDRO ENERGY DIVISION

Snorri Páll Kjaran
Jónas Elíasson

LEAKAGE FROM SIGALDA RESERVOIR

OS81018/VOD07
Reykjavík, September 1981

Prepared for
Landsvirkjun

ORKUSTOFNUN
NATIONAL ENERGY AUTHORITY
HYDRO ENERGY DIVISION
GRENSÁSVEGUR 9,
108 REYKJAVÍK ICELAND

Snorri Páll Kjaran
Jónas Elíasson

LEAKAGE FROM SIGALDA RESERVOIR

OS81018/VOD07
Reykjavík, September 1981

Prepared for
Landsvirkjun

ABSTRACT

The Króksvatn Reservoir is a part of the Sigalda Hydropower Plant and is created by building a dam across Sigalda Canyon. The dam is located at the upstream end of the canyon, the foundation and left abutment being built on postglacial lava. The southern bank of the reservoir basin is also formed of postglacial lava. The right abutment rests on a hyaloclastite (moberg) ridge covered with tillite, which is considered to be almost watertight.

The leakage from the reservoir proved to be somewhat larger than a priori estimates had expected. The leakage has been kept under close observation since 1976 by flow measurements in Sigalda Canyon and waterlevel observations in piezometer holes on the south bank area. The results of these measurements proved, rather surprisingly, to be a parabolic function of the reservoir level instead of a linear one, in contrast to classical groundwater theories. During impoundings of the reservoir, the formation of swallow holes, or sinks, was discovered in the submerged lava front of the south bank of the reservoir. Several sealing projects have been performed involving the placing of carpet seals over these swallow holes.

In analysing the problem, it proved necessary to separate the flow into two components, one component depending on the square of the reservoir level, and another linear one. Comparison with geolocial data succeeded in identifying the two components as largely separated flows in two contact scoria zones in the postglacial lava formation. It was also discovered, that the square component behavior of the associated flow was not due to large velocity values of the flow, but rather that during impoundings more and more swallow holes became active at the same time as the flow through them increased.

Final analysis of the flow was done in two finite element computer models, one for each component of the flow. The model predicts the flow in Sigalda Canyon and piezometer levels in the south bank area, as a function of the reservoir level. It also predicts a catchment loss, i.e. flow that does not appear again in the Sigalda Canyon but flows underground, out of the catchment area and is lost for power generation further down the

Tungnaá river. The total seepage loss at reservoir level 493 m a.s.l. is calculated to be 21 m^3/s whereof the catchment loss is 7 m^3/s but 14 m^3/s reappear in Sigalda Canyon.

LIST OF CONTENTS

LIST OF TABLES

LIST OF FIGURES

1 INTRODUCTION

In the beginning of the year 1979 Landsvirkjun (National Power Company) requested Orkustofnun (National Energy Authority) to carry out model calculations of the leakage from the Sigalda Reservoir on the basis of the extensive data that had been gathered (see P. Jóhannesson et al. 1978). In a letter to Landsvirkjun dated May 29th 1979 the main results of the Sigalda model calculations were presented.

These results indicated considerably higher leakage than earlier anticipated. In our letter of July 6th 1979 some explanations were given as well as recommendations for further investigations in the lava fields south-east of the reservoir (the long path leakage area). The hypothesis was put forward, that the Sigalda Ridge and an oval hill of móberg, 2 km to the southeast, were connected by a ridge of móberg at rather shallow depth below the lava surface. The existance of such an underground ridge of móberg, far less permeable than the lavas, lengthens the long leakage path which again diminishes the gradients and lessens the long path leakage discharge. It was decided to check this hypothesis by drillings. The drillhole data supported the hypothesis of a móberg ridge under the uppermost lava. The model calculations were repeated with new boundary conditions taking this móberg ridge into account. The results are given in this report.

In our letter of July 6th 1979 we pointed out the necessity of drilling piezometer holes along the long leakage path, in order to check the calculations. Two observation piezometer holes were therefore drilled together with the above mentioned drillings. Observations have however been insufficient to verify the calculations. It is therefore important to maintain continuous measurements in one of the piezometers.

The results have been discussed with Landsvirkjun representatives.

2 AVAILABLE DATA

The calculations are based on the large amount of data collected during the eight impoundings of the reservoir. The impounding history of the reservoir is shown in figs. 2 and 3. The measurements used are a) water level recordings in piezometer holes and b) flow measurements, at measuring weirs near the dam and discharge measurements in the almost dry Tungnaá River Canyon upstream of the Sigalda waterfall. These measurements are presented in a report by P. Jóhannesson et al. (1977) and several EWI/ Virkir reports. All our calculations are based upon stationary values, that is to say flow and water level values, when the reservoir has been stationary at the same level for a long time compared with the response time of the piezometers. The following measurements have been plotted vs. reservoir level:

A. Flow measurements

1. MW-1 (canal-measuring weir)
2. MW-2 (canal-measuring weir)
3. MW-3+MW-4 (canal-measuring weir)
4. Increased springflow, i.e. springflow measured in the Tungnaá Canyon minus flow in the canals and initial springflow.

B. Water level measurements for model calibration

1. PZ-15
2. PZ-16
3. PZ-17
4. PZ-18
5. PZ-19
6. PZ-20
7. E - 8
8. TK- 2
9. E -28

C. Water level measurements for model verification

1. SA- 2
2. SA- 3
3. VII
4. TK-12
5. VI
6. V
7. IX
8. PJ-11
9. PJ-12

The location of piezometers and flow measurement sites is shown in figs. 4 and 9. The piezometers mentioned under item B are used to calibrate the model, while the piezometers mentioned under item C are used for verification purposes in order to check the model calculations.

3 GEOLOGICAL FACTORS

A geological map of the model area is shown in fig. 1, which also indicates the probable extension of the Sigalda móberg at shallow depth. The southern banks of the reservoir are made of the socalled Th_h-lava layer, overlaying the Th_f-lava which covers most of the reservoir bottom. The Th_h-Th_f contact is at approx. 478 m a.s.l. and is rather scoriaceous, especially the lower part of the Th_h-lava. In the vicinity of the dam Th_c is overlain by the Th_f-lava, and the Th_f-Th_c contact has shown itself to be an effective aquifer.

The reservoir area is a former lake basin, with maximum water level at app. 500 m a.s.l. Clayish deposits of varying thickness have therefore covered the lavas and been deposited in the Th_h-Th_f contact, obviously because of leakage from the lake. A narrow strip along the Th_h-front is therefore tighter than the contact elsewhere, except perhaps in the Hnubbafossar area where the lavas are heavily eroded. Another erosion feature, the Sigalda canyon, later drained the old lake, and created numerous springs. There is no doubt that the disappearance of the old lake has caused a regional lowering of the groundwater table. This has the immediate effect, now the dam is built, and the lake restored without raising the groundwater table to its old level, that the clay deposits are subjected to greater differential pressures than before. This causes piping in the clay seal into cracks and cavities in the lava and the formation of swallow holes that increase in number when the water level is raised. Another effect of the emptying of the former reservoir lake has been surface water erosion in the reservoir bottom, particularly in the riverbed and on steep slopes like Th_h-lava front, creating conditions for infiltration and formation of swallow holes.

4 CANAL FLOW DATA

The flow in MW-1, the old diversion canal, is shown in fig. 5 vs. reservoir level. The relationship is seen to be linear. This flow comes from the Th_f-lava.

The flow in MW-2 is shown in fig. 6 vs. reservoir level. Before the 6th impounding there seems to be some square component in the flow, curving the data points to the right. At the 6th impounding the relationship is clearly linear again. Before the 6th impounding MW-2 had inflow from both the Th_f-lava and the Th_h-Th_f contact scoria. After the 5th impounding the inflow from the Th_h-Th_f contact scoria was diverted into MW-3 and MW-4 and thus just the Th_f-lava contributed to the flow in MW-2.

The flow in MW-3 and MW-4 is shown in fig. 7. Clearly both a linear and a square component are present in the flow, and field observations indicate clearly, that both of the canals have inflow from the Th_f-lava and the Th_h-Th_f contact scoria.

It can therefore be concluded that the canals have a linear flow component from the Th_f-Th_c contact scoria and a square flow component from the Th_h-Th_f contact scoria. Clearly the sealing work performed after the third impounding resulted in insignificant reduction of the canal flow.

5 SPRINGFLOW DATA

Increased springflow is shown in fig. 8. It can be shown that the increased springflow varies with the square of the reservoir water level height above 478 m a.s.l. This result is in agreement with the canal analysis indicating that the square component originates from the Th_h-Th_f contact scoria. According to the flow measurements the sealing work has significantly reduced this flow. This result is incompatible with the piezometer level data as discussed in ch. 8.

6 PIEZOMETER LEVEL DATA

Location map for the piezometers used in the analysis is shown in fig. 9. Stationary values for the piezometer level vs. reservoir level is shown in figs. 10-18. The piezometer level is the potential head of the Th_h, Th_f and Th_c-lavas. The relationship between the reservoir level and the piezometers seems to include the same square and linear components found in the relationship between the reservoir level and the flow measurements. There seems to be some evidence that the sealing work has actually reduced the rise in the piezometer levels, but this indication is considerably less than might be expected from the increased springflow measurements, see fig. 8.

In the following we write the piezometer level of the form:

$$h-h_o = k_2(H-478)^2+k_1(H-476.5)$$

The zero level, h_o, is shown in fig. 9 and the constants k_2 and k_1 are shown in figs. 45-48.

7 DATA ANALYSIS

To establish a relationship between the flow data and the piezometer level data that is compatible with the geological factors, it is necessary to separate and explain separately the linear and square components. Although the permeability is great in the area the gradients are very small; thus a turbulent flow model explaining the square component in the piezometer level is not possible. Fig. 19 shows stationary values for the piezometer level in E-28 vs. flow in the canyon. The relationship is seen to be linear in the form

$$Q = 2.196\ h - 1046.829$$

with a correlation coefficient of 0.995. The regional groundwaterflow is therefore likely to follow Darcy's law, and turbulent flow model is thus not possible. It can be seen from the above equation that one meter difference in piezometer level gives 2.2 m^3/s difference in flow values. The inflow from the reservoir into the Th_h-Th_f contact scoria is mostly due to swallow holes formed by the differential pressure on the clayish bottom deposits. Therefore both linear and square flow components exist as the following analysis explains. The water level in the piezometers is proportional to nQ, where n is the number of swallow holes and Q is the inflow into each one. Q is again proportional to H-h, where H is the reservoir height and h the piezometer height above the Th_h-Th_f contact level. The simplest relationship for n is $n \sim H$. We therefore have $h \sim H$ (H-h), that is:

$$h = \frac{\delta}{1+\delta H} \cdot H^2,$$

which can be approximated by $h = k_2 \cdot H^2$. The formulas of the straight lines and parabolas fitted to the measured flow values and shown in figs. 5-8 are listed in table 1. The respective coefficients for the piezometer parabolas are shown in figure 9 and figures 45 to 48. The reference level 478 m a.s.l., used in the formula, is the level of the Th_h-Th_f contact scoria, see ch. 2. The reference level 476.5 m a.s.l. is the lake level when the groundwater gradients from the reservoir to the aquifer are reversed.

TABLE 1 Measured flow values (m^3/s)

BEFORE SEALING WORK		
Initial springflow	:	4.5
Increased springflow	:	$0.04869(H-478)^2$
MW-3+MW-4	:	$0.01044(H-478)^2+0.1639(H-476.5)$
MW-2	:	$0.12166(H-476.5)$
MW-1	:	$0.0845(H-476.5)$
Total square	:	$0.05913(H-478)^2$
Total linear	:	$0.3701(H-476.5)$
AFTER SEALING WORK		
Initial springflow	:	4.5
Increased springflow	:	$0.02486(H-478)^2$
MW-3+MW-4	:	$0.01044(H-478)^2+0.1639(H-476.5)$
MW-2	:	$0.12166(H-476.5)$
MW-1	:	$0.0845(H-476.5)$
Total square	:	$0.0353(H-478)^2$
Total linear	:	$0.3701(H-476.5)$

H: reservoir water level in m a.s.l.

8 NUMERICAL MODELING

It has been seen that the inflow/outflow is written in the form

$$Q-Q_o = C_2(H-478)^2+C_1(H-476.5)$$

and the piezometerlevel in the form

$$h-h_o = k_2(H-478)^2+k_1(H-476.5).$$

The only mathematical solution to this problem is that k_1 and k_2 correspond to C_1 and C_2 respectively. We have therefore determined the necessary distribution of the inflow/outflow from the area to match the linear and square components in the piezometer level. For this purpose Laplace's equation is solved with the appropriate boundary conditions in a finite element grid numerical computer model. For the sake of simplicity the permeability of the area is assumed constant. The Laplace equation is solved twice, once for the linear and square flow components respectively. The finite element grid is shown in fig. 20 and 21 with the appropriate boundary conditions. The boundary condition in Sigalda Canyon is the so called spillway boundary condition given by:

$$T \frac{\delta h}{\delta h} = \alpha h$$

where T is the transmissivity, $\frac{\delta h}{\delta h}$ the gradient, h the piezometric level and α a proportionality constant. Fig. 19 confirms this boundary condition. In order to establish the remaining boundary conditions the boundary piezometers are analysed. The time variations of the boundary piezometers for eight impoundings of the reservoir are shown in figs. 22-33. Comparing these figures with the impounding history, figs. 2 and 3, reveals the following:

a) The boundary piezometers in the west, II, III and IV are seen to depend on the reservoir level. The boundary conditions in the two lava passes in the west are thus considered two unknown boundary outflow values.

b) The two boundary piezometers in the south, TH-10, TH-11, are seen to be independent of the reservoir level. The piezometric level in TH-10 is more dependent on natural groundwater inflow than reservoir level. The boundary condition in the southern lavapass is thus considered a no flow boundary.

c) The boundary condition at the lake is considered an unknown inflow boundary. The móberg formations are considered to be watertight.

From the boundary piezometric level data the constants k_1 and k_2 for II, III and IV are determined and given in the following table.

TABLE 2 Piezometer constants for boundary piezometers

Piezometers / Piezometer constants	II	III	IV
k_1	0	$3.39 \cdot 10^{-2}$	$1.53 \cdot 10^{-2}$
k_2	$1.00 \cdot 10^{-2}$	$5.48 \cdot 10^{-3}$	$5.42 \cdot 10^{-3}$

If there is a 10 m rise in reservoir level the piezometric level rises 10 k_1 meters according to the linear flow and 100 k_2 meters according to the square flow. Estimation of the constants from the available boundary piezometric data was very difficult owing to paucity of measurements and lack of information as to the natural flow variations. In the following we therefore use the constants between limits defined by

$$0 \leq k \leq \beta \cdot k_{table}$$

where β is some constant.

In the case of the linear flow component we take the reservoir inflow to consist of two unknown inflow values, see fig. 45 and 46. According to former geological investigations the Th_f-lava was not found in boundary piezometer II. Therefore it is assumed that the extension of the Sigalda móberg closes this lavapass off completely. The outflow values in the two passes in the west therefore consist of two unknown outflow values for the square flow, but only one unknown for the linear flow. We therefore have three (four) unknown flow values. These unknown flow values are determined by matching the measured and calculated piezometric levels in such a way that the following norm is minimized.

$$L = \Sigma(k_1^{measured} - k_1^{calculated})^2$$

where L is the norm to be minimized, the summation is taken over the number of boreholes and $k_1^{measured}$ and $k_1^{calculated}$ is the linear constant from measurements and calculations respectively.

The minimum value of L is known as the residual norm. The unknown boundary outflow parameter, α, in the Sigalda Canyon is now determined by minimizing the residual norm. The result is now shown in figs. 34, 40, 41, 45 and 46. As mentioned above the k values for the boundary piezometers II, III and IV are very uncertain. The sensitivity of the results is now investigated with respect to the parameter β defined above. The result is given in fig. 35, which shows the residual norm increasing rapidly for β greater than one.

We then select the most probable β interval to be $0 \leq \beta \leq 1$. Fig. 36 shows catchment loss divided by measured loss against β, since β lies between zero and one we have

$$1.7 \leq {}^{\text{Catchment loss}}/_{\text{Measured loss}} \leq 1.8$$

where catchment loss is the outflow in the lava passes in the west, and measured loss is the measured flow in Sigalda Canyon minus the initial springflow and the flow in MW-1 and MW-2.

The same procedure is now repeated for the square flow component. The minimum α-value is shown in fig. 37 and the piezometric level in figs. 42, 43, 47 and 48. The β interval is determined from fig. 38 to be $0 \leq \beta \leq 1$. Fig. 39 then gives for the catchment square flow loss.

$$0.30 \leq {}^{\text{Catchment loss}}/_{\text{Measured loss}} \leq 0.50.$$

The result for the combined effect of linear flow and square flow components at lake level 493 m a.s.l. is shown in figs. 44 and 49.

The flow under the dam is not included in the calculations, but taken to correspond to the flow in MW-1 and MW-2.

In order to check the results the water level measurements mentioned in ch. 1C are used for model verification. The comparison between measured and calculated piezometric level is shown in figs. 50-56.

These water level measurements were not used for model calibration but for verification of the model. The figures show good correlation between the two sets.

9 RESULTS

The reservoir inflow can be separated into a linear component and a square component. The linear component is believed to be flow in the Th_f-lava at the dam and leakage in the Th_h-Th_f contact scoria at Hnubbafossar.

Heavy drainage of groundwater towards the canyon keeps the groundwater level low in the lavas while the reservoir level rises thus causing increased differential pressure on the clay deposits on the submerged lava fronts. The square component is most likely swallow hole leakage in the Th_h-lava, when the reservoir clay succumbs to differential water pressure. Bearing this in mind the main conclusion to be drawn from the calculations are:

1) The spring flow in the Tungnaá River Canyon is mainly governed by the regional ground water level. Seasonal variations of the groundwater level are therefore crucial when comparing reservoir leakage before and after each impounding. The sealing work in 1977, aimed at stopping the swallow-hole leakage (the square component), did not succeed as expected. This can be seen from fig. 57. Here we also have the greatest discrepancy between the model and the flow measurements. According to the model the sealing work would have decreased the swallow-hole leakage by about 10%, but springflow measured in the Tungnaá River Canyon after the operation indicates a decrease of about 50%. Since the model is based on the piezometric measurements, there is a discrepancy in the relationship between the piezometric measurements and the above mentioned reduction of the springflow. It can also be seen from fig. 8 that early summer impoundings always give more increased springflow than late summer impoundings. In our opinion the reason for this discrepancy is the seasonal variation in the undisturbed natural groundwater level.

In early summer impoundings the natural groundwater level is higher than during autumn impoundings. Different natural groundwater levels cause different springflow, which is estimated to be a constant equal to 4.5 m^3/s; although it is of course higher when natural groundwater level is high and lower when natural groundwater level is low. The difference between the increased springflow measurements in the third and fourth impounding at reservoir level 490 is 3 m^3/s, (fig. 8). According to fig. 19 this corresponds to a difference in piezometer level in E-28 of 1.4 m. The actual difference in natural groundwater levels between impoundings 3 and 4 may have been in the region of one meter.

It is therefore not possible to estimate the effect of the sealing work by comparing early summer and autumn flow measurements or even by comparing different years, without knowing the undisturbed regional natural groundwater level. It should also be pointed out that the square component inflow of the area now covered by the sealing carpet was about one order of magnitude larger than the rest of the inflow (see fig. 47). Therefore the location of the sealing carpet was correctly chosen.

2) The model predicts leakage figures. The following notations have been used for the different leakage values.

Measured loss:	Measured flow in Sigalda Canyon. Fig. 58.
Catchment loss:	Calculated flow out of the catchment area through the two lava passes in the southwest. Fig. 59.
Total loss:	Sum of the measured loss and the catchment loss. Fig. 60.

The model predicts significant loss figures, as shown in fig. 60, which gives both the total loss and the measured loss. It can be seen that the measured loss is about 2/3 of the total loss, and the catchment loss is about 1/3 of the total loss. The loss figures are given between two limits according to the above mentioned limits in the calculations. The catchment loss is greatly influenced by the behaviour of the piezometric level in the southern part of the area, where information is very scarce. SA-2 and SA-3 were drilled in order to improve the situation, but owing to the paucity of measurements they have not been as useful as expected. It is therefore very important to maintain continuous registration of the water level in either SA-2 or SA-3 in order to be able to check the calculations better.

3) The model determines the regional permeability in the area to be of the order of 40-60 cm/sec. This is in fair agreement with the previously determined permeabilities. In P. Jóhannesson et al. 1978 the permeability is estimated from temperature measurements to be in the interval of 10-70 cm/s. By using the results of the tracing tests performed in the summer of 1980 (see EWI/Virkir 1980) the corresponding permeability can be approximated to be at least in the order of 10 cm/s.

4) The optimum energy reservoir level vs. reservoir inflow is calculated from the model results and given in fig. 61. Three curves are shown in fig. 61. The first gives the optimum energy reservoir level if the leakage consisted only of the measured loss, while the other two give the limits of optimum energy reservoir level for total leakage figures. The limits correspond to the above defined limits for flow values. The calculations are based upon constant efficiency and take only the power output from Sigalda into account. Calculations are now in progress which will take Hrauneyjafoss and Búrfell into consideration with the assumption that the catchment loss is irretrievable for power generation at Hrauneyjafoss and Búrfell.

REFERENCES

Electrowatt/Virkir 1978: Test impounding to 494 m a.s.l. and supplement to report: "Impounding conditions, sealing and drainage work to be undertaken during 1978". Landsvirkjun, 10 s.

Electrowatt/Virkir 1978: Report on the 6th impounding to el. 495 m September/October 1978. Landsvirkjun, 9 s.

Electrowatt/Virkir 1979: Report on the 7th impounding to el. 496,5 m May/June 1979. Landsvirkjun, 5 s.

Electrowatt/Virkir 1980: Present reservoir conditions and recommended remedial measures. Landsvirkjun, (60) s.

Electrowatt/Virkir 1980: Summary of main findings from the tracing tests summer 1980. Landsvirkjun, (22) s.

Pálmi Jóhannesson, Sigurður St. Arnalds, Davíð Egilson & Bjoern Jónasson 1978: Summary of impounding data until November 1977 and reevaluation of the hydrogeological conditions (Vol. I & II). Landsvirkjun, 78 s. + 88 m.

ÁGRIP (abstract in Icelandic)

Reiknaður er leki úr lóni Sigölduvirkjunar. Frá árinu 1976 hefur verið fylgst mjög vel með lekanum með rennslismælingum í Sigöldugljúfri og vatnshæðarmælingum í borholum á svæðinu. Við athugun á þessum mælingum kom í ljós að bæði rennslið og vatnshæðin í borholum eru háð lónhæðinni í öðru veldi. Það reyndist því nauðsynlegt að skipta rennslinu í tvo þætti, einn sem væri línulega háður lónhæðinni og annan sem væri háður lónhæðinni í öðru veldi. Með aðstoð jarðfræðinnar var hægt að tengja þessa tvo rennslisþætti tveimur vatnsleiðurum í hraununum. Það kom ennfremur í ljós að rennslisþátturinn, sem var háður lónhæðinni í öðru veldi er ekki tilkominn vegna iðustreymis, heldur vegna svelgjamyndunar á hraunkantinum, þegar svelgjum fjölgar við hækkandi lónstöðu.

Við reikninga á lekanum var notuð bútaaðferð Galerkins og stillt upp líkani fyrir hvorn rennslisþátt fyrir sig. Líkanið reiknar síðan rennsli í Sigöldugljúfri og vatnshæð í borholum á svæðinu. Ennfremur er reiknað tap út af vatnasviði og er það leki, sem ekki kemur fram í Sigöldugljúfri, og nýtist sennilega ekki til orkuframleiðslu á Landsvirkjunarsvæðinu. Lekinn er fall af lónhæð og er því meiri sem hærra er í lóninu. Leki við lónhæð 493 m y.s. reiknaðist 21 m^3/s. Þar af tapast 7 m^3/s út af vatnasviðinu, en 14 m^3/s renna út í Sigöldugljúfur.

FIGURES

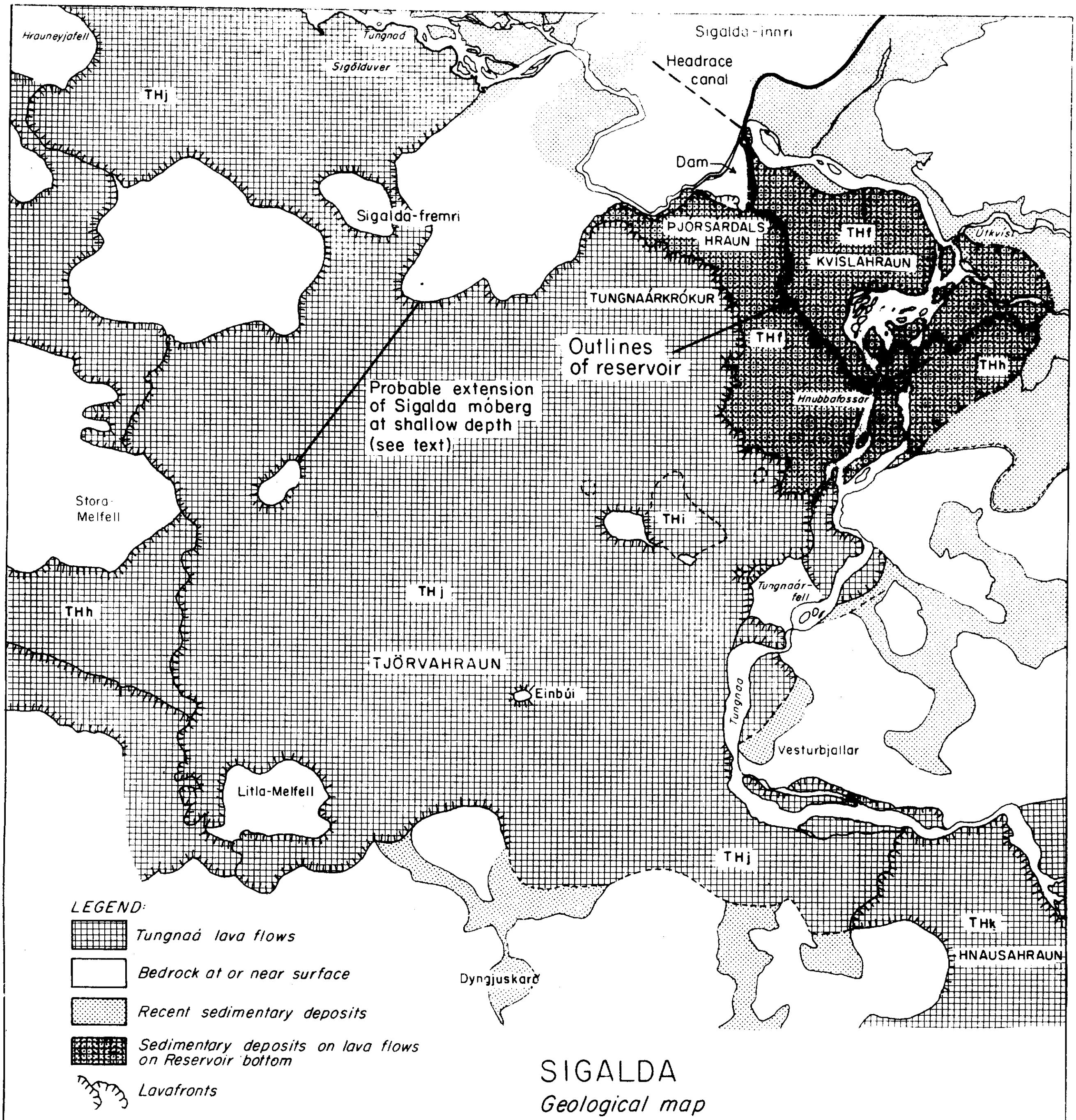

Fig. I

SIGALDA
Geological map

'80.09.01. SPK/ÓD B-332 F-19952

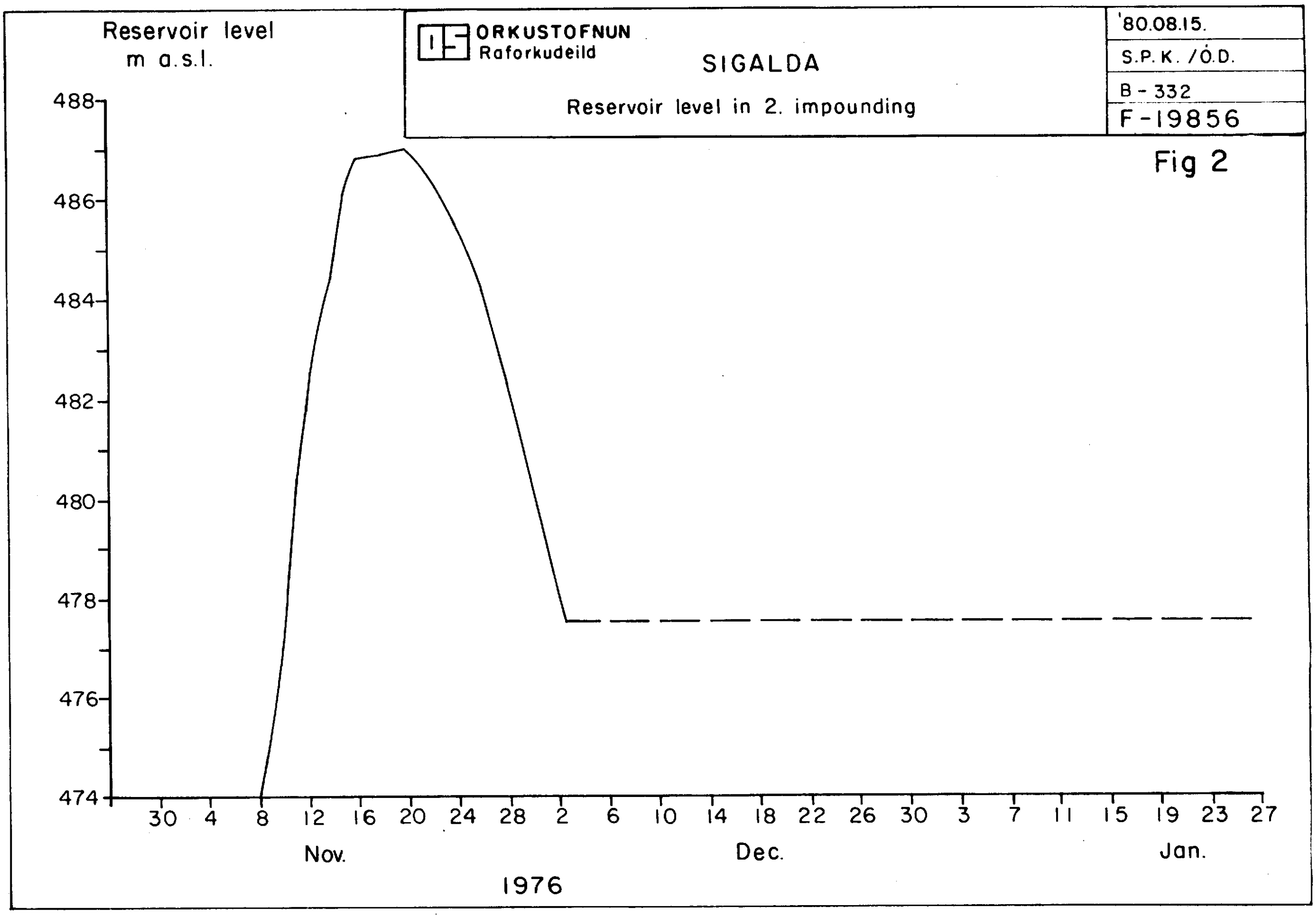
Reservoir level
m a.s.l.
ORKUSTOFNUN
Raforkudeild
SIGALDA
Reservoir level in 2. impounding
'80.08.15.
S.P.K. /Ó.D.
B - 332
F-19856
488
486
484
482
480
478
476
474
30 4 8 12 16 20 24 28 2 6 10 14 18 22 26 30 3 7 11 15 19 23 27
Nov.
Dec.
Jan.
1976
Fig 2

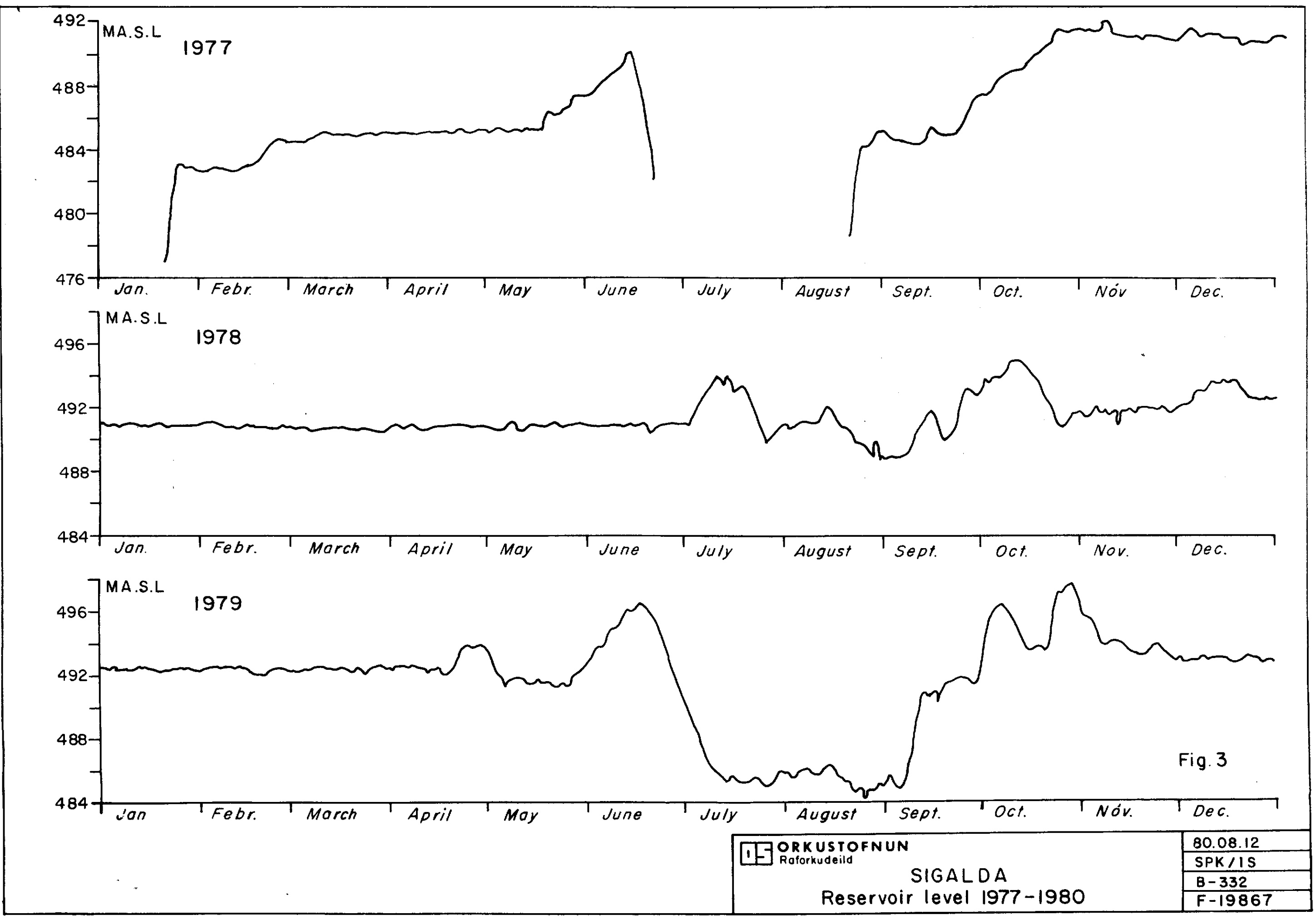
MA.S.L
1977
492
488
484
480
476
Jan. Febr. March April May June July August Sept. Oct. Nov Dec.
MA.S.L
1978
496
492
488
484
Jan. Febr. March April May June July August Sept. Oct. Nov. Dec.
MA.S.L
1979
496
492
488
484
Jan Febr. March April May June July August Sept. Oct. Nov. Dec.
Fig. 3

ORKUSTOFNUN
Raforkudeild
SIGALDA
Reservoir level 1977-1980
80.08.12
SPK/IS
B-332
F-19867

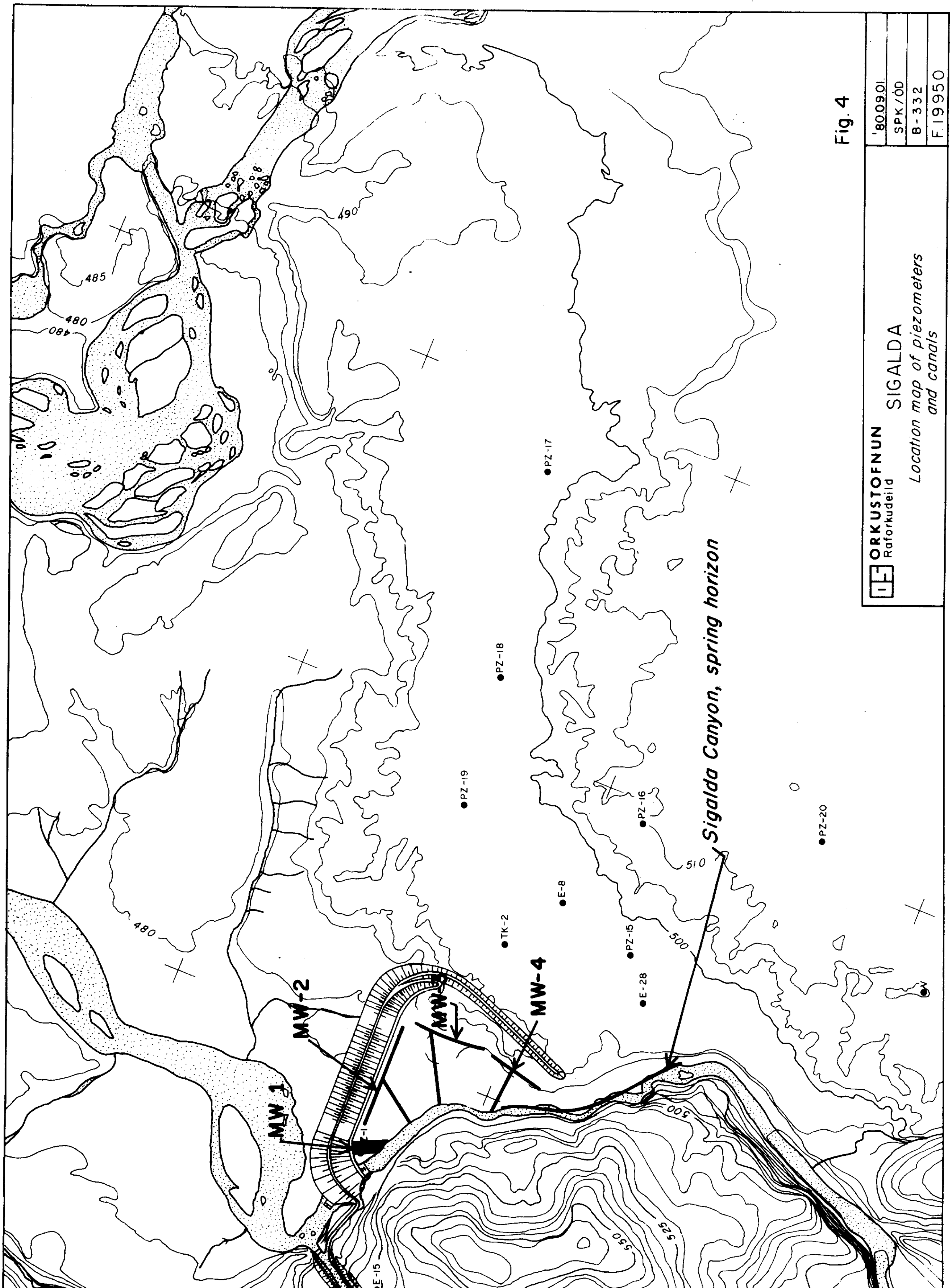
Fig. 4
'80.09.01
SPK/ÖD
B-332
F 19950
ORKUSTOFNUN
Raforkudeild
SIGALDA
Location map of piezometers and canals
Sigalda Canyon, spring horizon
MW-1
MW-2
MW-3
MW-4
PZ-15
PZ-16
PZ-17
PZ-18
PZ-19
PZ-20
E-8
E-15
E-28
TK-2
480
485
490
500
510
525
550

ORKUSTOFNUN
Raforkudeild

SIGALDA

MW-1 *Discharge vs. Reservoir level*

1979 04 26
D.E./Ó.D.
B-332
F. 18389

Fig. 5

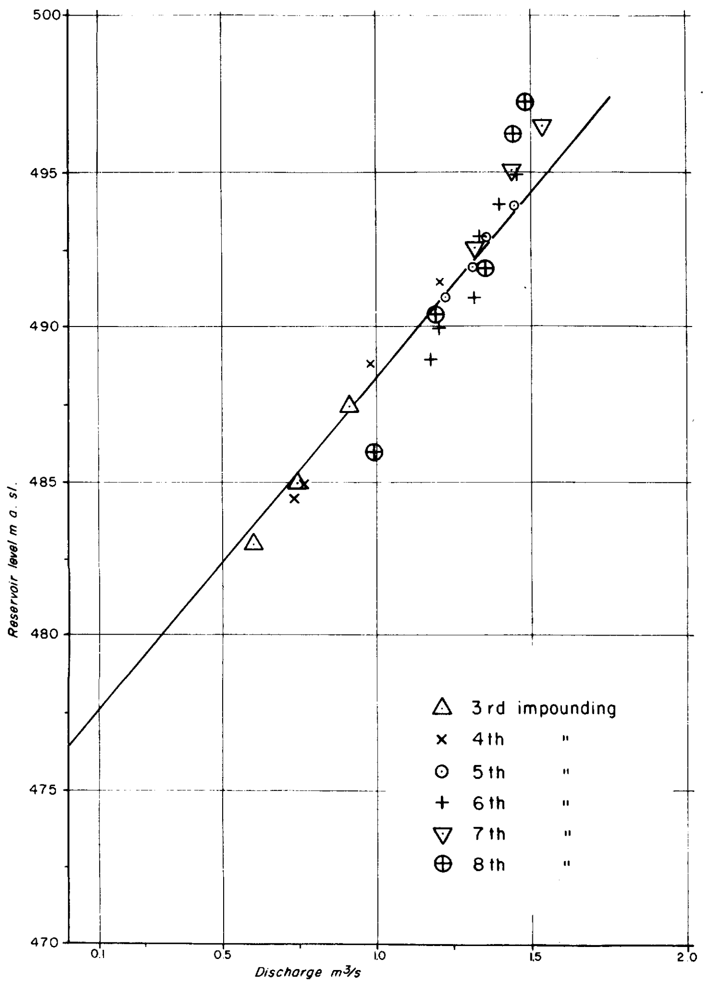

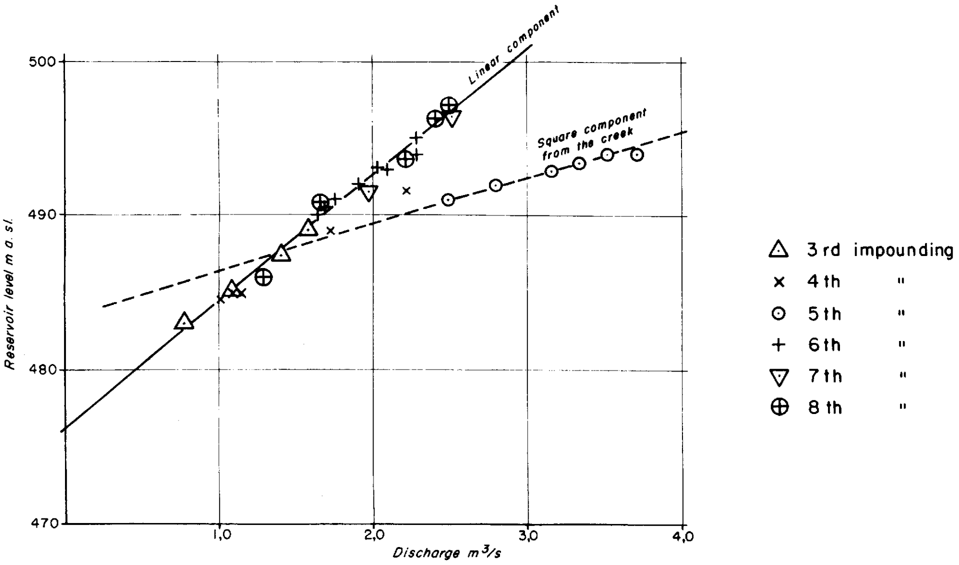

Fig. 6

ORKUSTOFNUN
Raforkudeild

SIGALDA

MW-2 *Discharge vs. Reservoir level.*

1979 04 26
D.E./Ó.D.
B-332
F. 18391

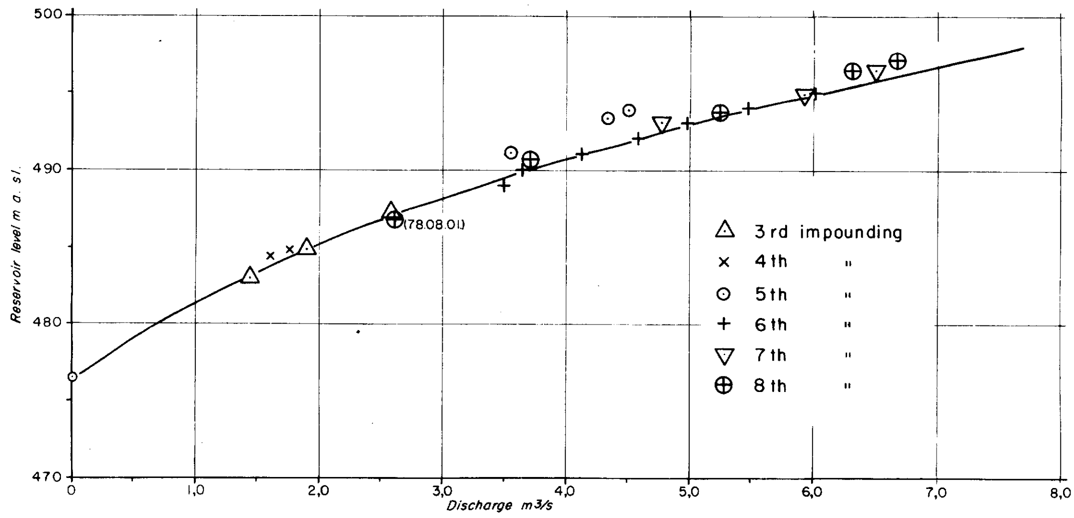

Fig. 7

ORKUSTOFNUN
Raforkudeild
SIGALDA
MW-3 and MW-4 vs. Reservoir level
1979 04 26
D.E./Ó.D.
B-332
F.18390

ORKUSTOFNUN
Raforkudeild
SIGALDA
Increased springflow vs. Reservoir level
1979 04 26
D.E./Ó.D.
B-332
F.18387

Fig. 8

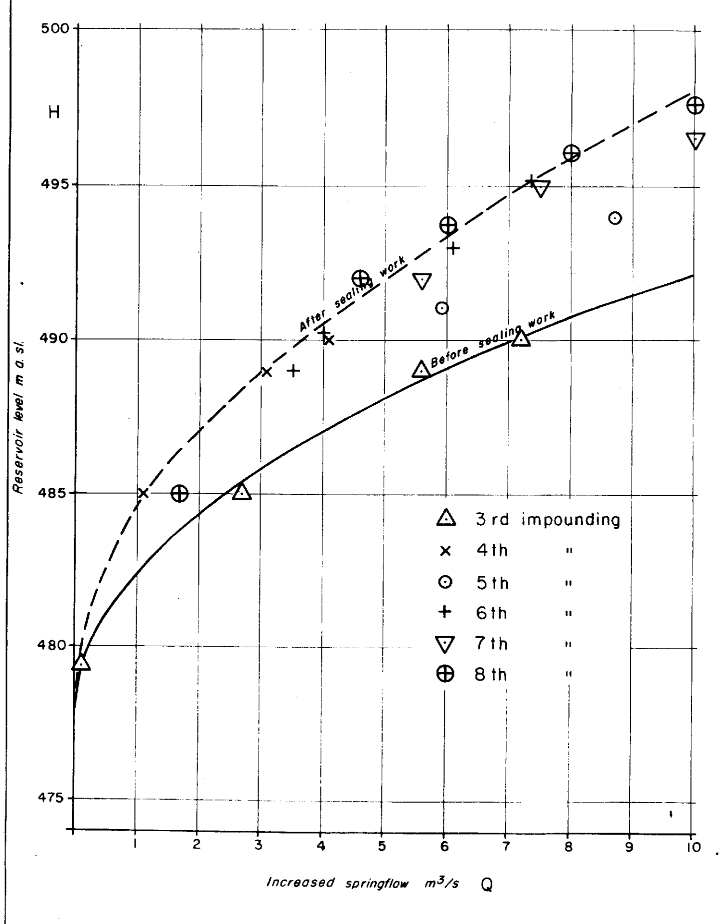

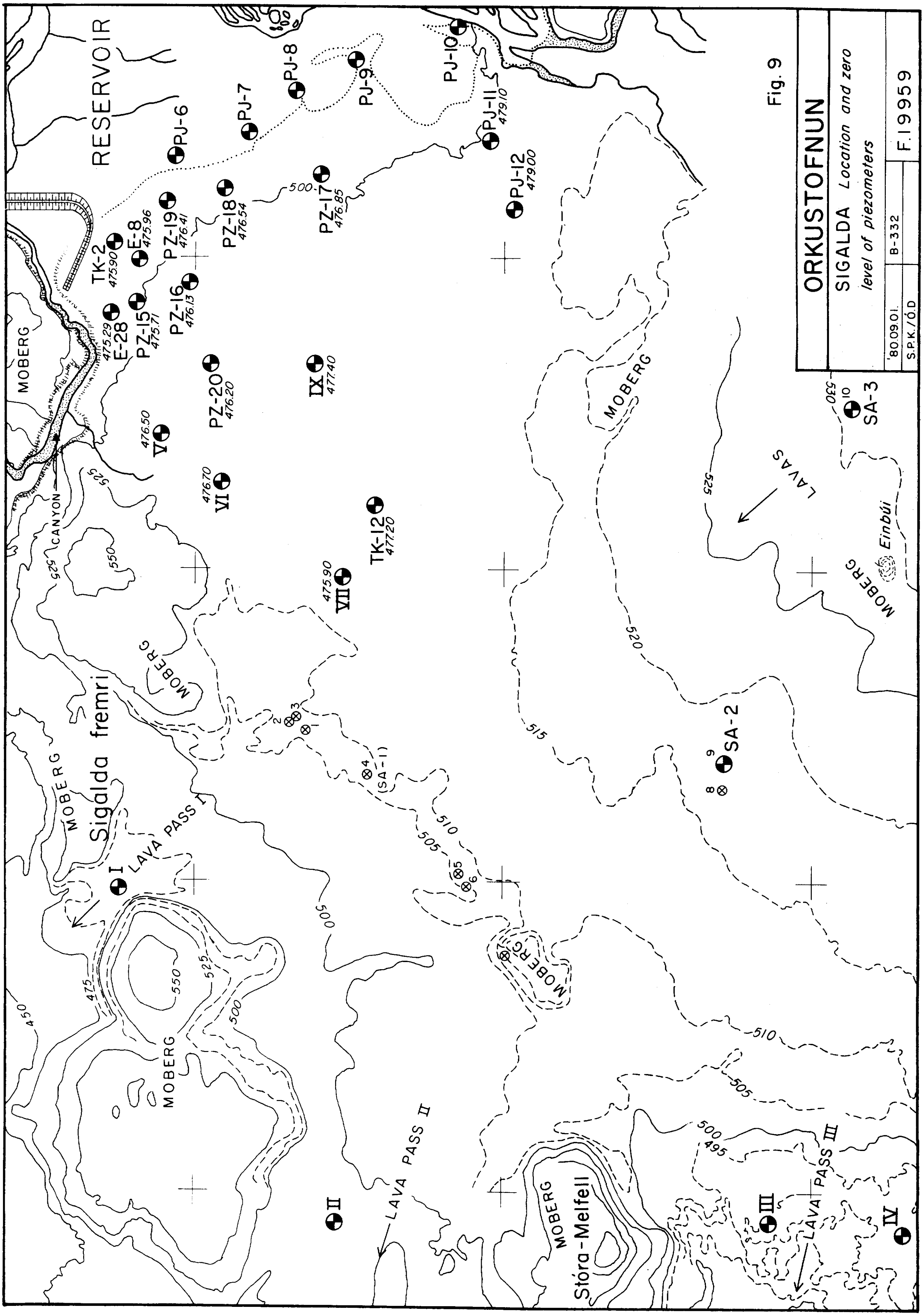
ORKUSTOFNUN
SIGALDA Location and zero level of piezometers
'80.09.01.
S.P.K./Ó.D
B-332
F.19959
Fig. 9
RESERVOIR
PJ-6
PJ-7
PJ-8
PJ-9
PJ-10
PJ-11 479.10
PJ-12 479.00
PZ-17 476.85
PZ-18 476.54
PZ-19 476.41
E-8 475.96
TK-2 475.90
PZ-16 476.13
PZ-15 475.71
E-28 475.29
PZ-20 476.20
IX 477.40
V 476.50
VI 476.70
TK-12 477.20
VII 475.90
CANYON
MOBERG
Sigalda fremri
LAVA PASS I
LAVA PASS II
LAVA PASS III
(SA-1)
SA-2
SA-3
LAVAS
Einbúi
Stóra-Melfell
I
II
III
IV
450
475
500
505
510
515
520
525
530
550

ORKUSTOFNUN Raforkudeild | SIGALDA PZ-16 VS. RESERVOIR LEVEL | 1979 04.25 DE/Gyða B-332 F. 18386

Fig. 10

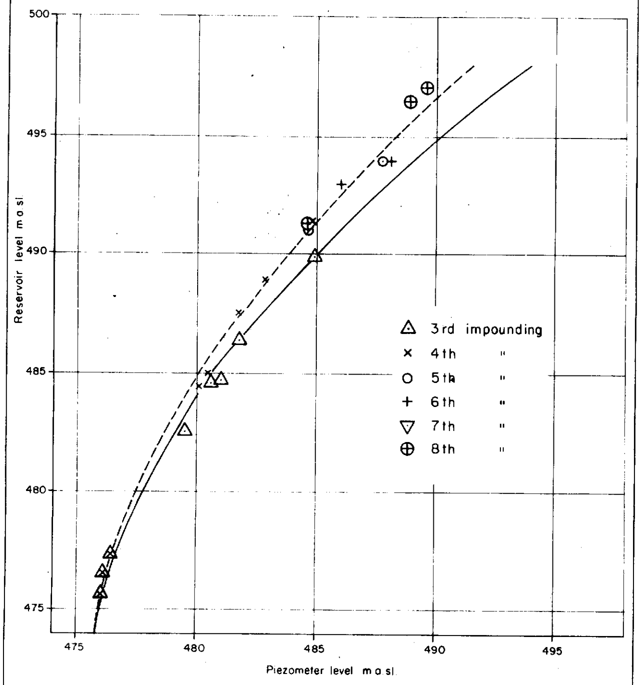

ORKUSTOFNUN Raforkudeild | SIGALDA TK-2 VS. RESERVOIR LEVEL | 1979 04.25 DE/Gyða B-332 F-18385

Fig. 11

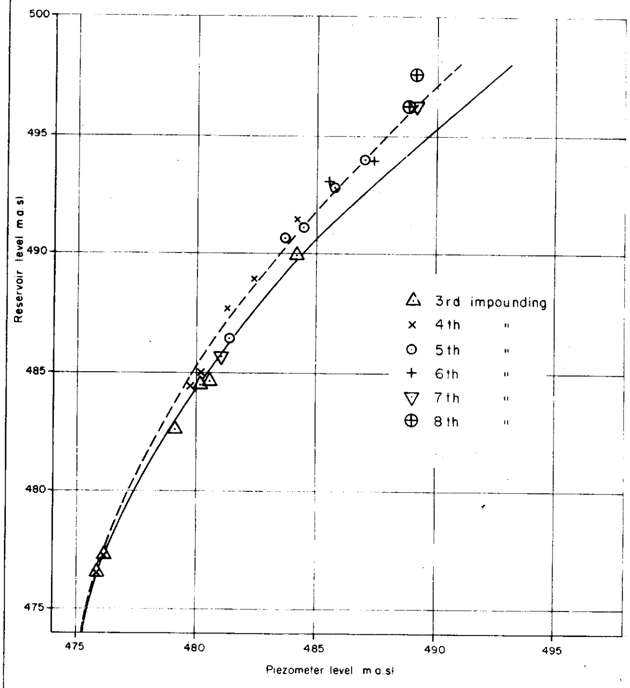

ORKUSTOFNUN Raforkudeild | SIGALDA E-28 VS. RESERVOIR LEVEL | 1979 04.25. DE/Gyða B-332 F-18384

Fig. 12

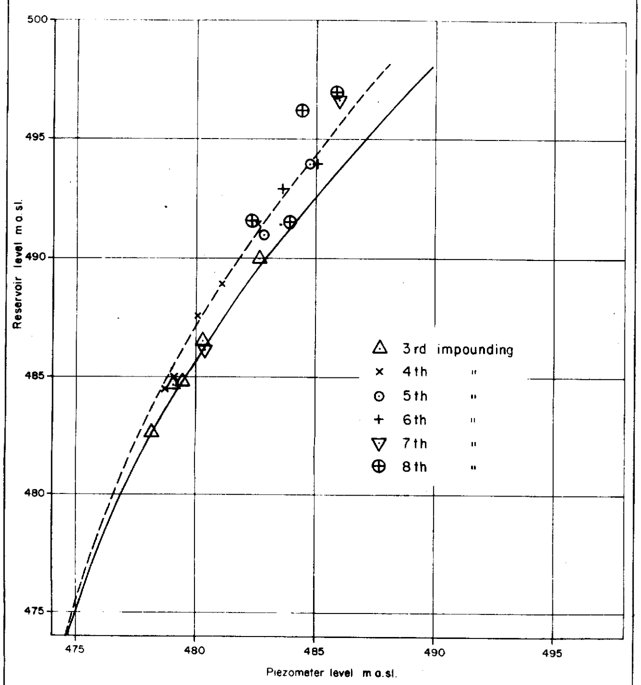

ORKUSTOFNUN Raforkudeild | SIGALDA E-8 VS. RESERVOIR LEVEL | 1979 04.25 DE/Gyða B-332 F-18383

Fig. 13

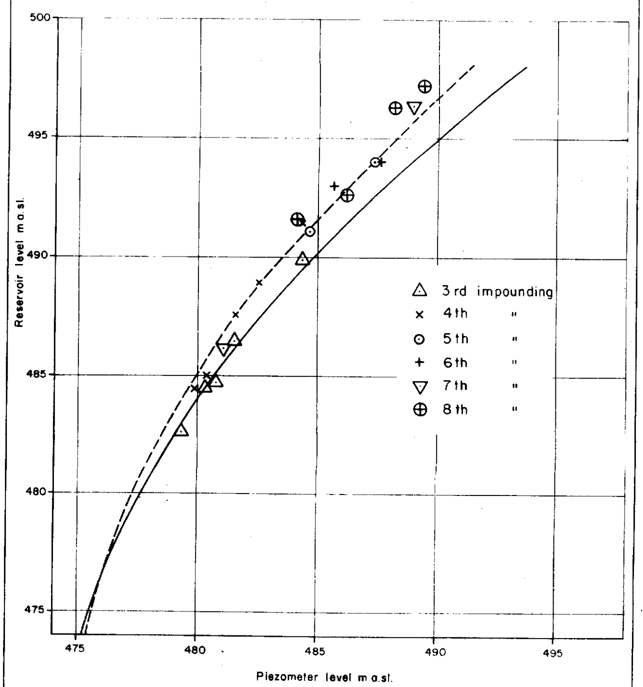

ORKUSTOFNUN Raforkudeild | SIGALDA PZ-17 VS. RESERVOIR LEVEL | 1979 04 25 DE/Gyða B-332 F-18382

Fig. 14

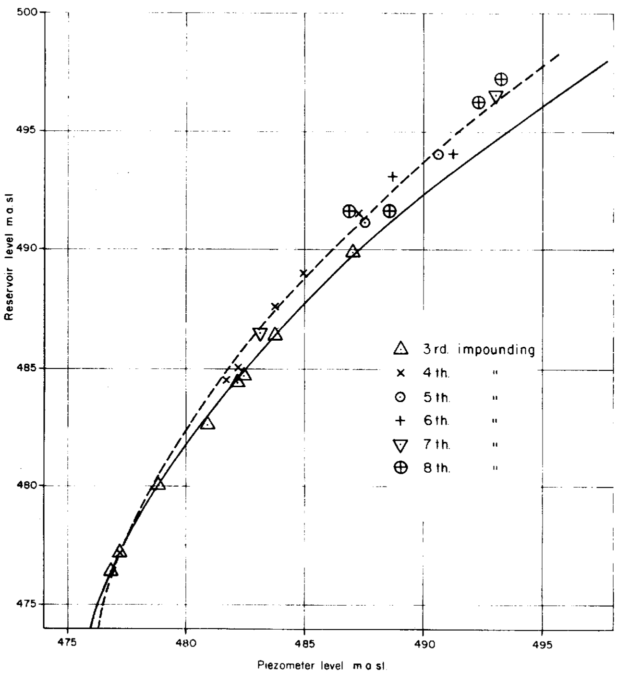

ORKUSTOFNUN Raforkudeild | SIGALDA PZ-20 VS. RESERVOIR LEVEL | 1979 04 25 DE/Gyða B-332 F-18381

Fig. 15

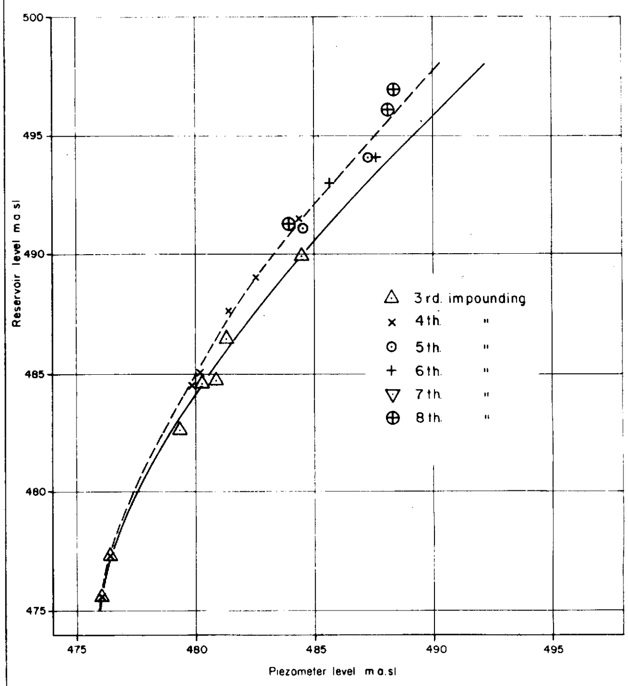

ORKUSTOFNUN Raforkudeild | SIGALDA PZ-19 VS. RESERVOIR LEVEL | 1979 04 25 DE/Gyða B-332 F-18380

Fig. 16

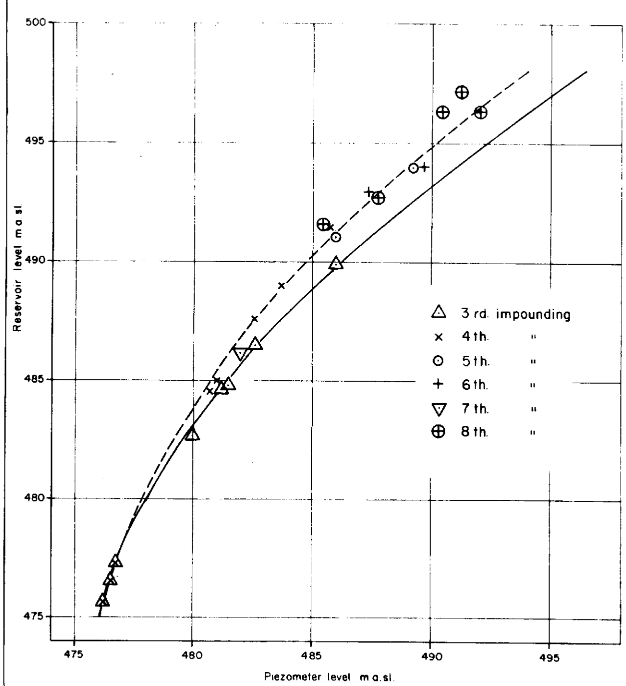

ORKUSTOFNUN Raforkudeild | SIGALDA PZ-18 VS. RESERVOIR LEVEL | 1979 04 25 DE/Gyða B-332 F-18379

Fig 17

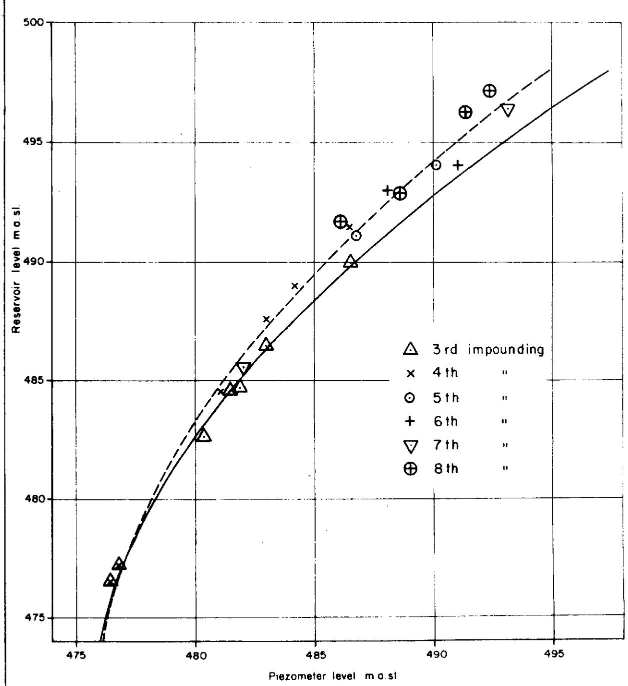

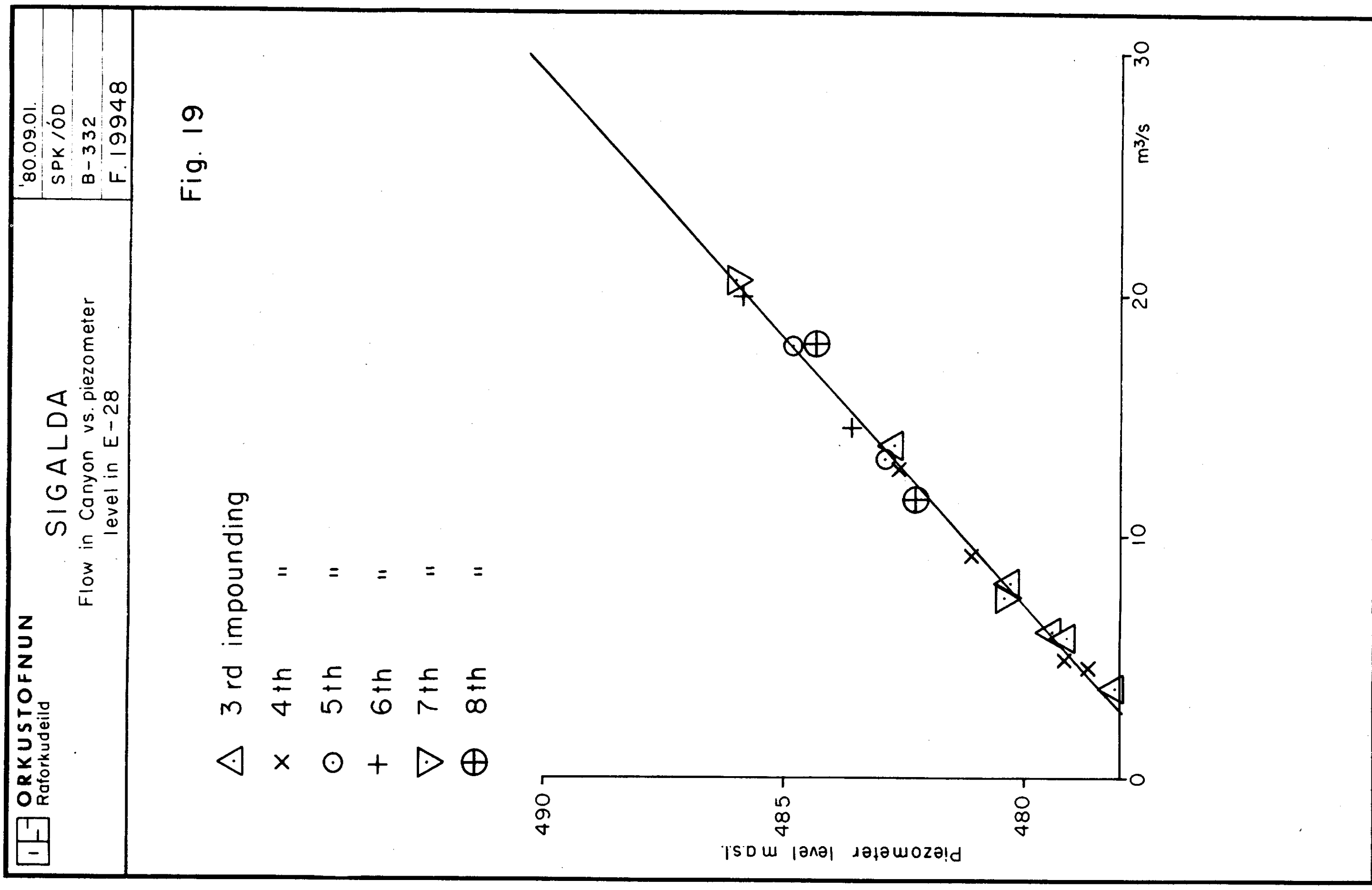
ORKUSTOFNUN
Raforkudeild
SIGALDA
Flow in Canyon vs. piezometer level in E-28
'80.09.01.
SPK/ÓD
B-332
F.19948
3 rd impounding
4 th "
5 th "
6 th "
7 th "
8 th "
Piezometer level m.a.s.l.
490
485
480
0
10
20
30
m³/s
Fig. 19

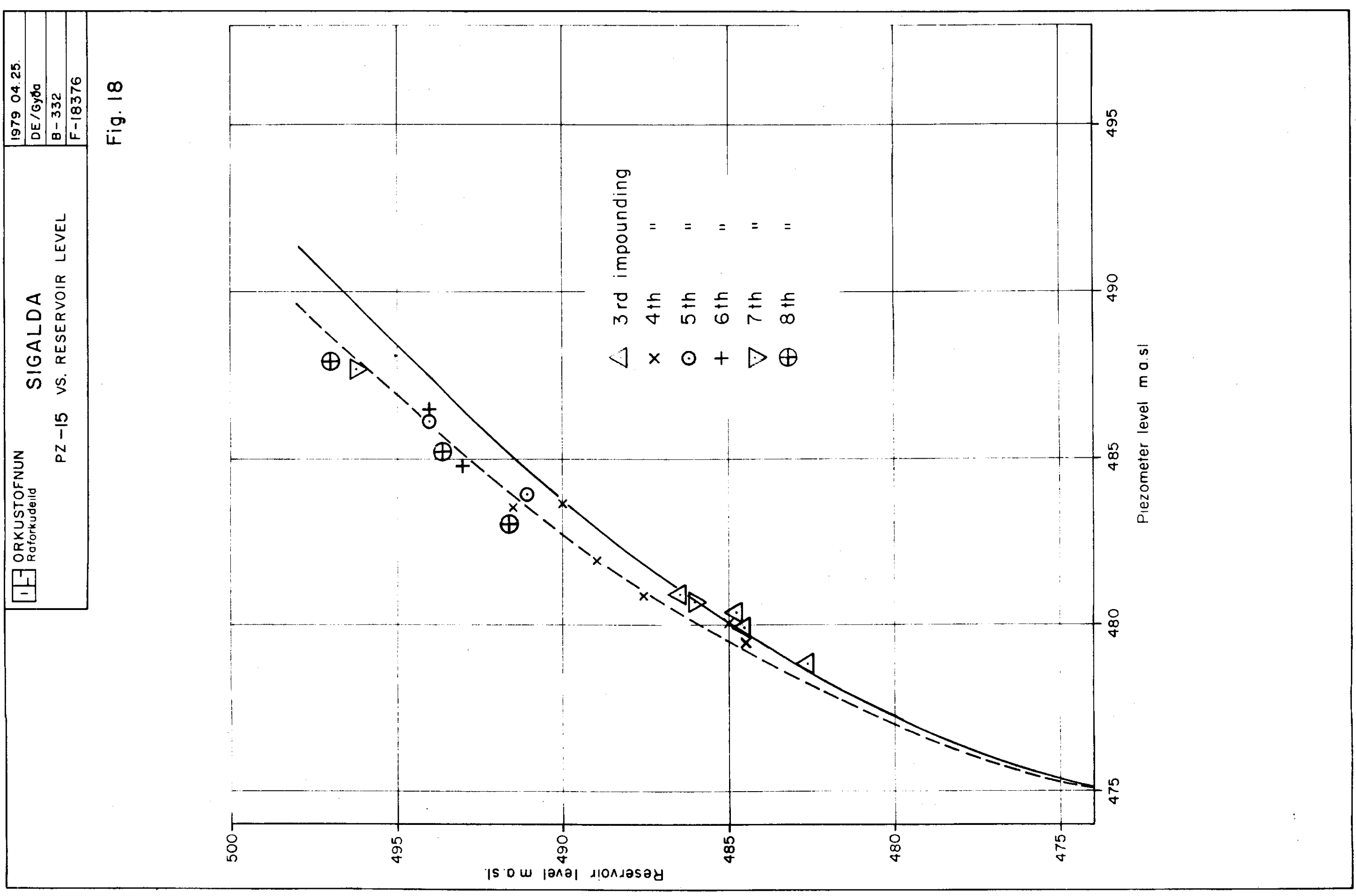
ORKUSTOFNUN
Raforkudeild
SIGALDA
PZ-15 VS. RESERVOIR LEVEL
1979 04.25.
DE/Gyða
B-332
F-18376
3rd impounding
4th "
5th "
6th "
7th "
8th "
Reservoir level m.a.sl.
500
495
490
485
480
475
Piezometer level m.a.sl
475
480
485
490
495
Fig. 18

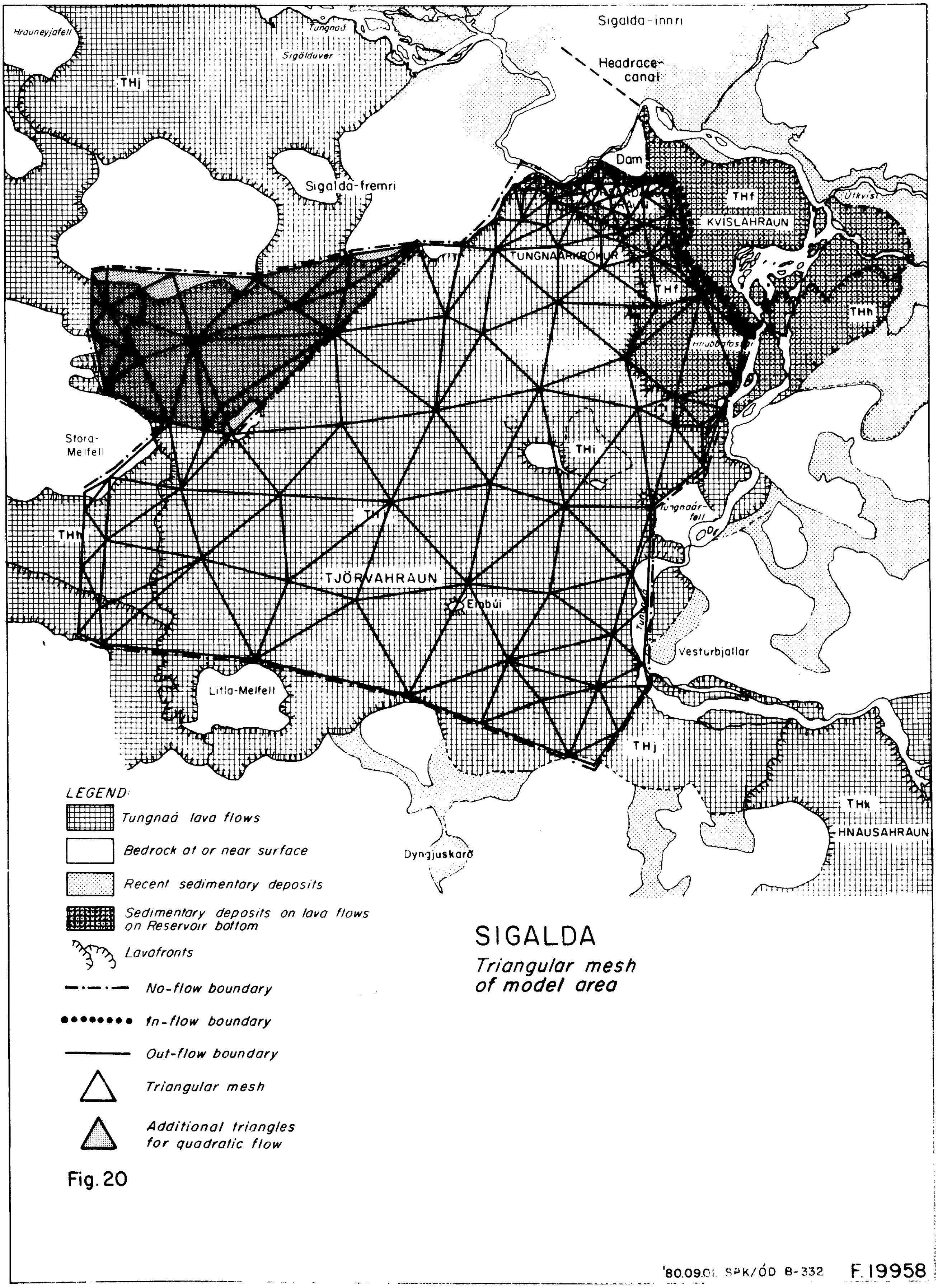
Hrauneyjafell
Tungnaá
Sigölduver
Sigalda-innri
Headrace-canal
THj
Dam
Sigalda-fremri
THf
KVISLAHRAUN
Útkvísl
TUNGNAÁRKRÓKUR
THf
THh
Stora-Melfell
THi
Tungnaár-fell
THh
TJÖRVAHRAUN
Embúi
Vesturbjallar
Litla-Melfell
THj
Dyngjuskarð
THk
HNAUSAHRAUN
LEGEND:
Tungnaá lava flows
Bedrock at or near surface
Recent sedimentary deposits
Sedimentary deposits on lava flows on Reservoir bottom
Lavafronts
No-flow boundary
In-flow boundary
Out-flow boundary
Triangular mesh
Additional triangles for quadratic flow
SIGALDA
Triangular mesh of model area
'80.09.01 SPK/ÓD B-332 F.19958

Fig. 20

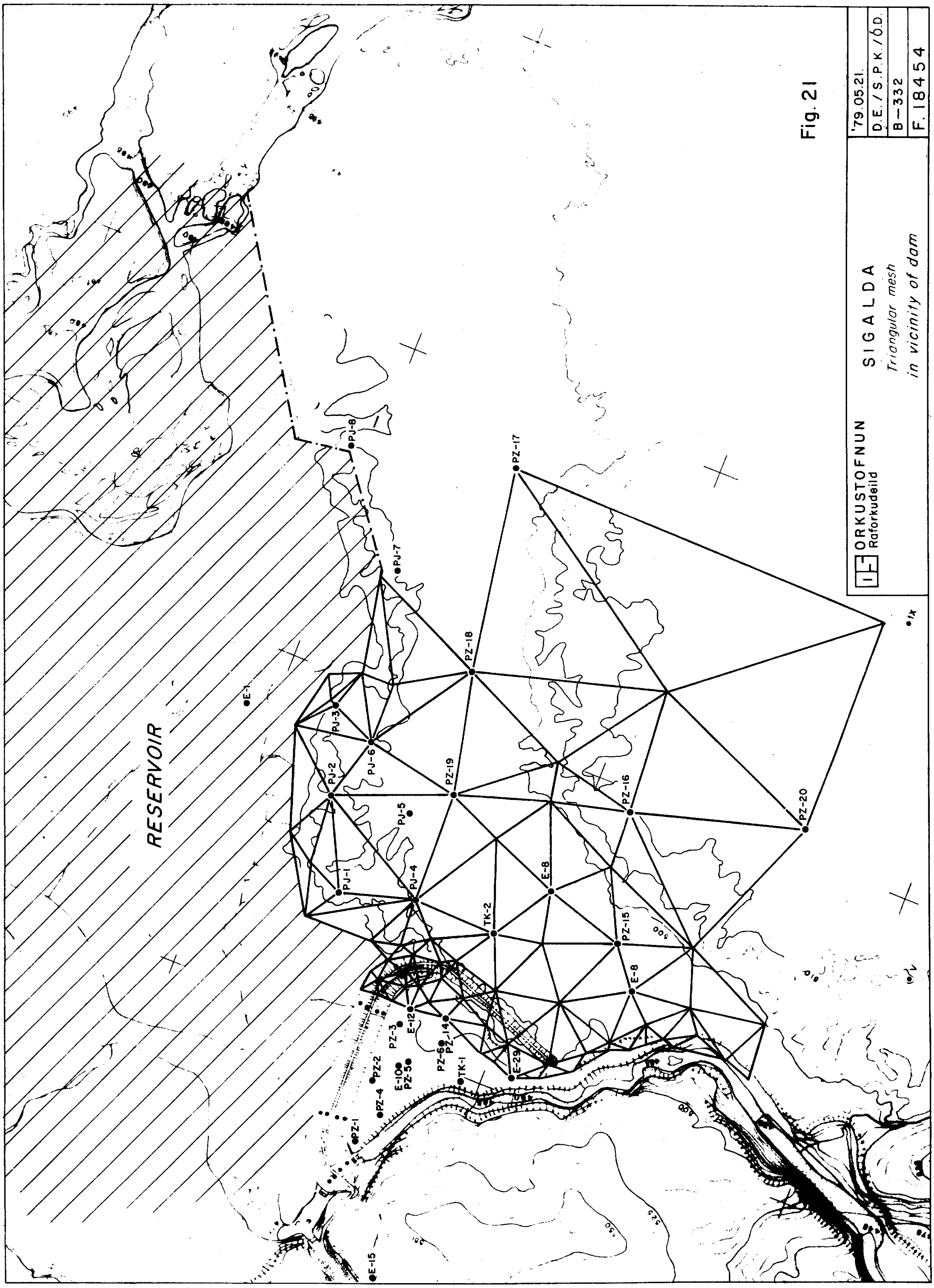
RESERVOIR
PJ-1
PJ-2
PJ-3
PJ-4
PJ-5
PJ-6
PJ-7
PJ-8
PZ-1
PZ-2
PZ-3
PZ-4
PZ-5
PZ-6
PZ-14
PZ-15
PZ-16
PZ-17
PZ-18
PZ-19
PZ-20
E-1
E-8
E-10
E-12
E-15
E-29
TK-1
TK-2
500
ORKUSTOFNUN
Raforkudeild
SIGALDA
Triangular mesh
in vicinity of dam
'79.05.21.
D.E./S.P.K./Ó.D.
B-332
F.18454
Fig. 21

ORKUSTOFNUN
Raforkudeild

SIGALDA

Boundary piezometer level in 2. impounding.

'80.08.12.
SPK/EBF
B-332
F-19856

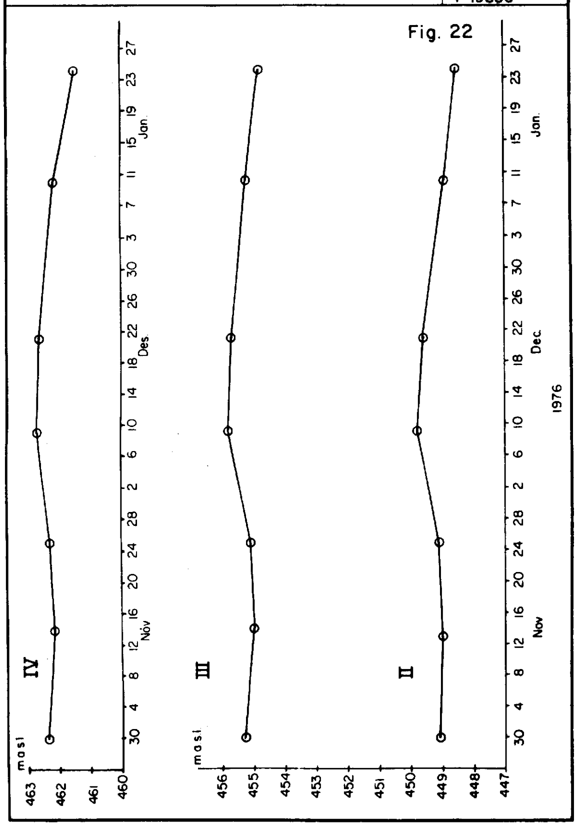

Fig. 22

ORKUSTOFNUN
Raforkudeild

SIGALDA

Boundary piezometer level in 2. impounding.

'80.08.12
SPK/EBF
B-332
F-19854

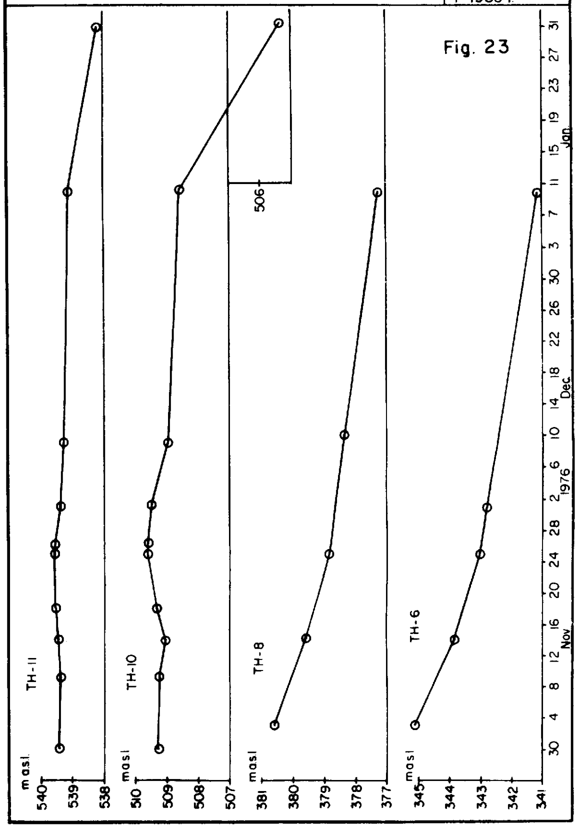

Fig. 23

ORKUSTOFNUN
Raforkudeild

SIGALDA

Boundary piezometer level in 3. impounding.

'80.08.12.
SPK/EBF
B-332
F-19857

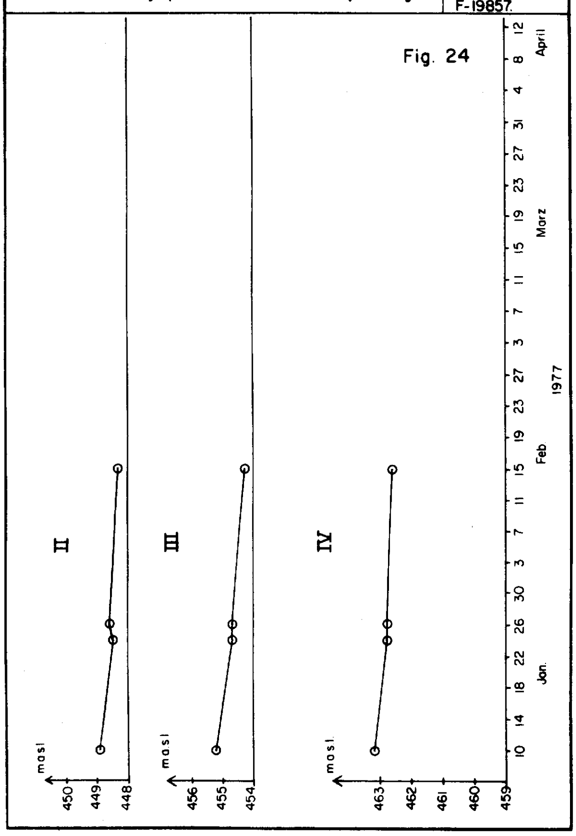

Fig. 24

ORKUSTOFNUN
Raforkudeild

SIGALDA

Boundary piezometer level in 3. impounding.

'80.08.12
SPK/EBF
B-332
F-19858

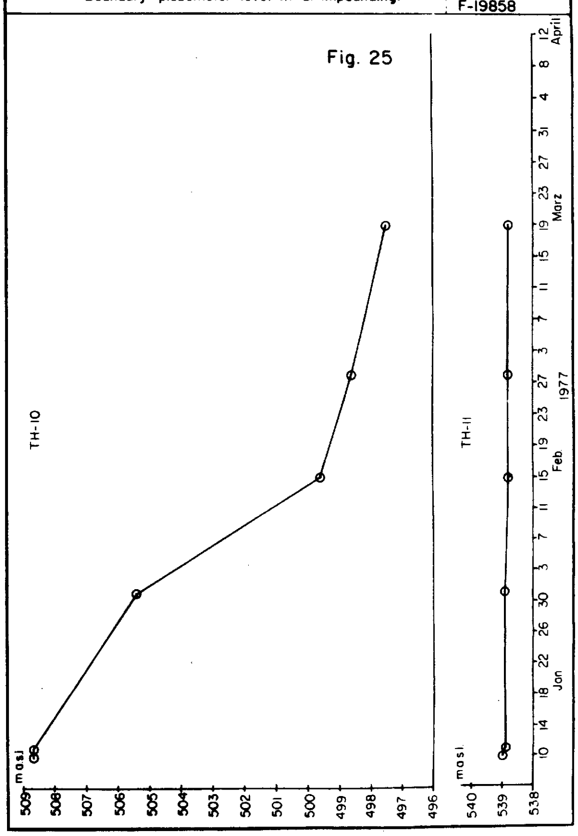

Fig. 25

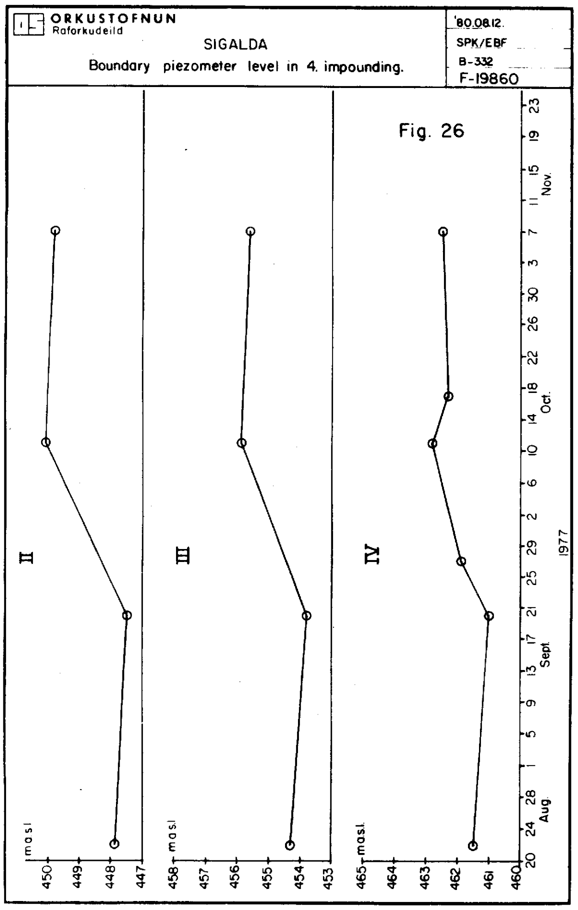
ORKUSTOFNUN
Raforkudeild
SIGALDA
Boundary piezometer level in 4. impounding.
80.08.12.
SPK/EBF
B-332
F-19860
Fig. 26
II
III
IV
m a s l
1977
Aug
Sept.
Oct.
Nov.

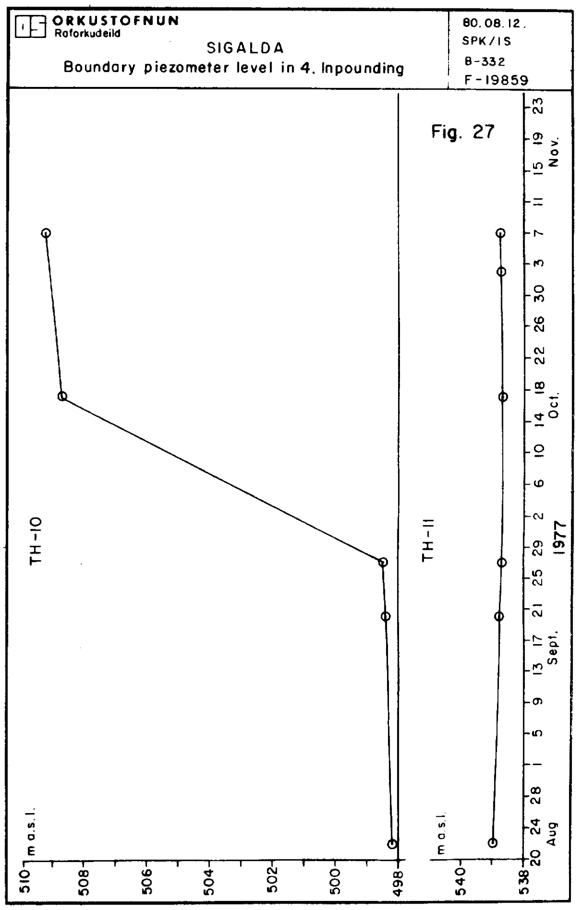
ORKUSTOFNUN
Raforkudeild
SIGALDA
Boundary piezometer level in 4. Inpounding
80.08.12.
SPK/IS
B-332
F-19859
Fig. 27
TH-10
TH-11
m a.s.l.
1977
Aug
Sept.
Oct.
Nov.

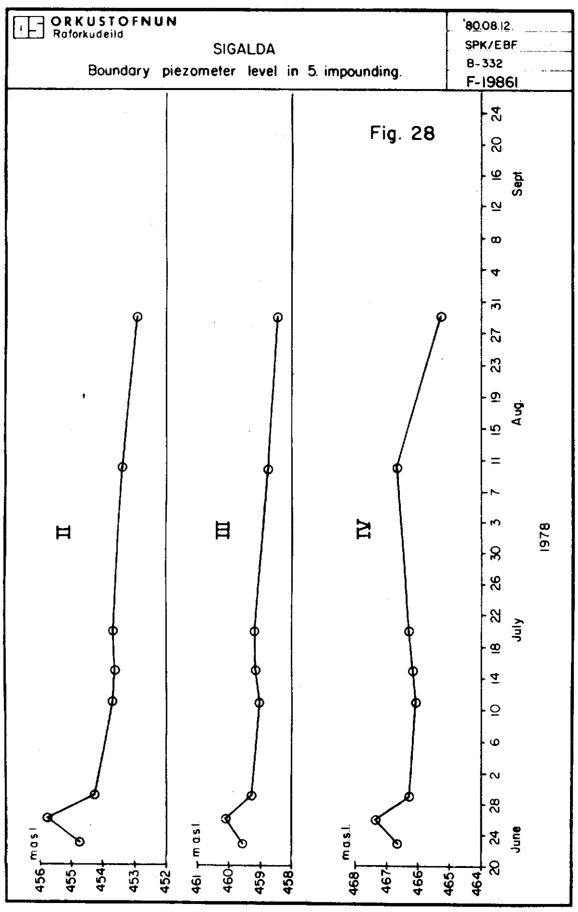
ORKUSTOFNUN
Raforkudeild
SIGALDA
Boundary piezometer level in 5. impounding.
80.08.12.
SPK/EBF
B-332
F-19861
Fig. 28
II
III
IV
m a s l
1978
June
July
Aug.
Sept.

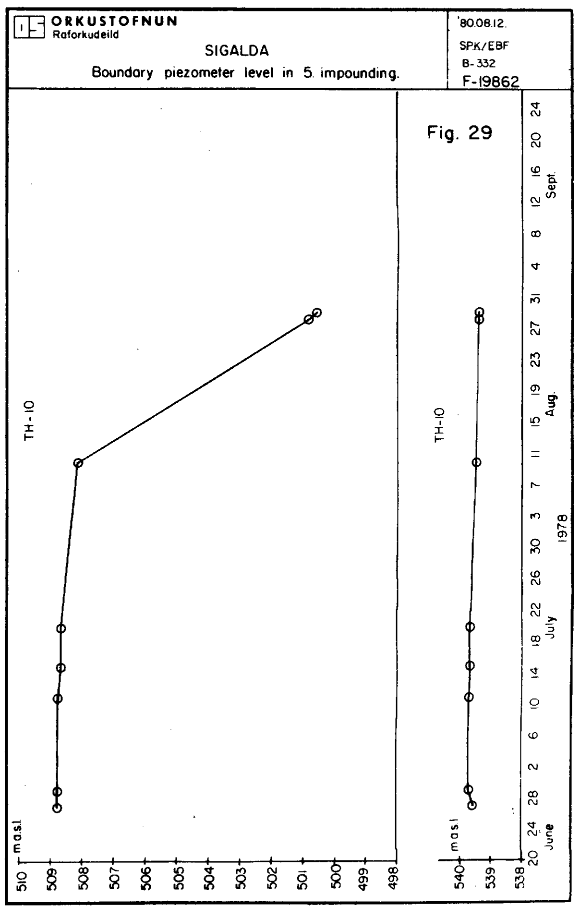
ORKUSTOFNUN
Raforkudeild
SIGALDA
Boundary piezometer level in 5. impounding.
80.08.12.
SPK/EBF
B-332
F-19862
Fig. 29
TH-10
TH-10
m a s l
1978
June
July
Aug.
Sept.

ORKUSTOFNUN
Raforkudeild

SIGALDA
Boundary piezometer level in 6. Inpounding

80.08.12.
SPK/IS
B-332
F-19863

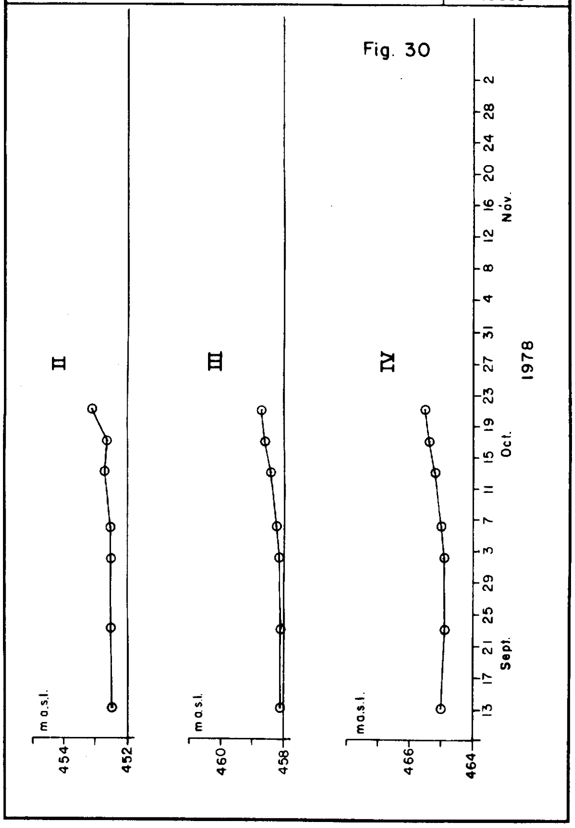

Fig. 30

ORKUSTOFNUN
Raforkudeild

SIGALDA
Boundary piezometer level in 6. Inpounding

80.08.12
SPK/IS
B-332
F-19866

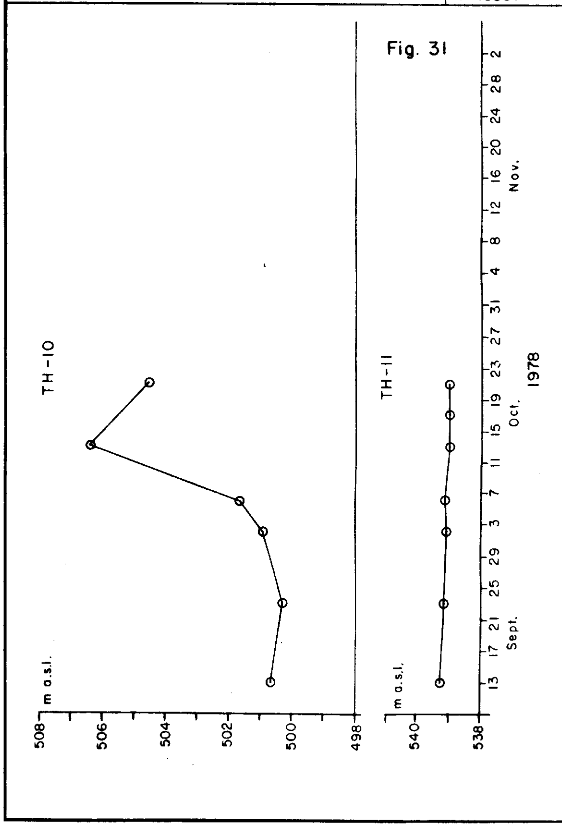

Fig. 31

ORKUSTOFNUN
Raforkudeild

SIGALDA
Boundary piezometer level in 8. inpounding.

80.08.12.
SPK/EBF
B-332
F-19865

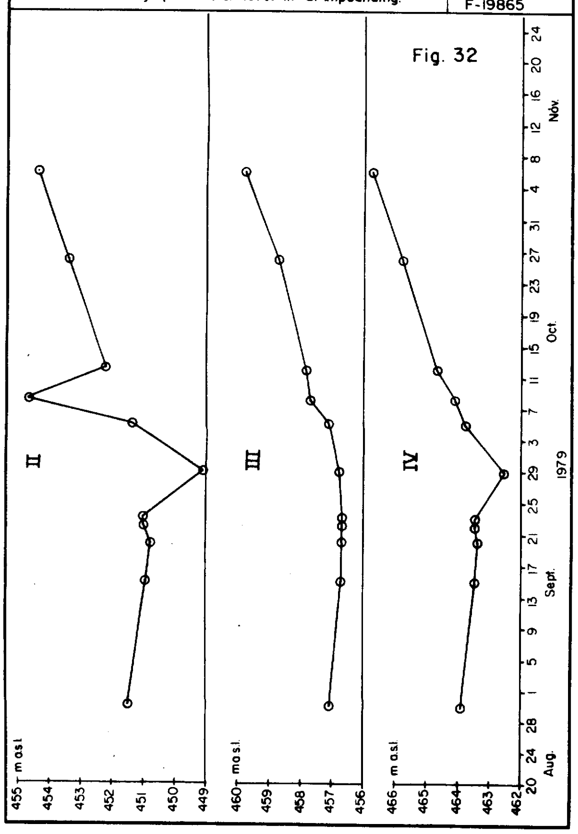

Fig. 32

ORKUSTOFNUN
Raforkudeild

SIGALDA
Boundary piezometer level in 8. inpounding

80.08.12
SPK/IS
B-332
F-19866

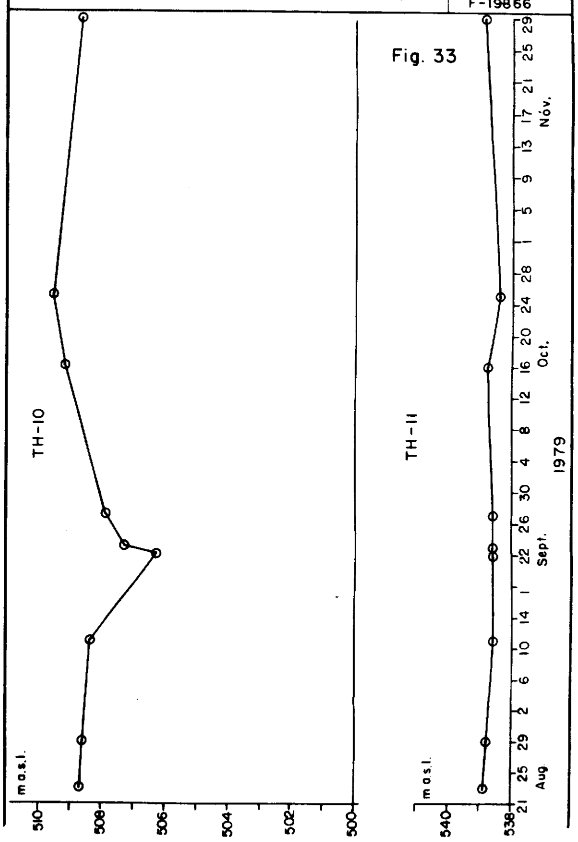

Fig. 33

ORKUSTOFNUN
Jarðhitadeild

SIGALDA
Linear flow component
Boundary flow parameter α vs. residual norm

80.07.29.
SPK / GSJ
B-332
F. 19833

Fig. 34

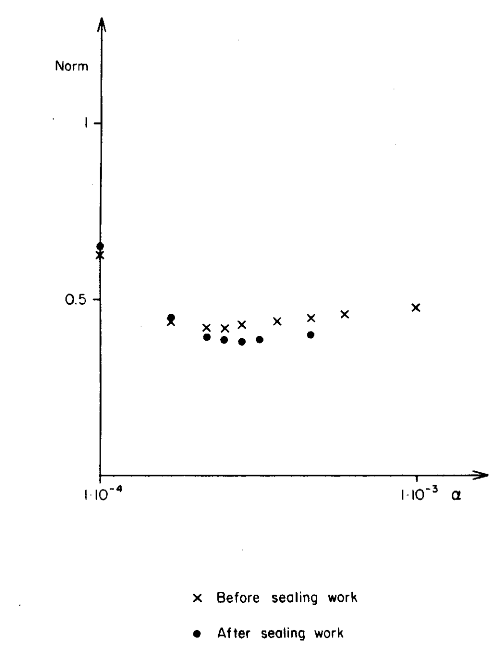

ORKUSTOFNUN

SIGALDA
Linear flow component β
vs. residual norm

80.07.29.
SPK / GSJ
B-332
F. 19832

Fig. 35

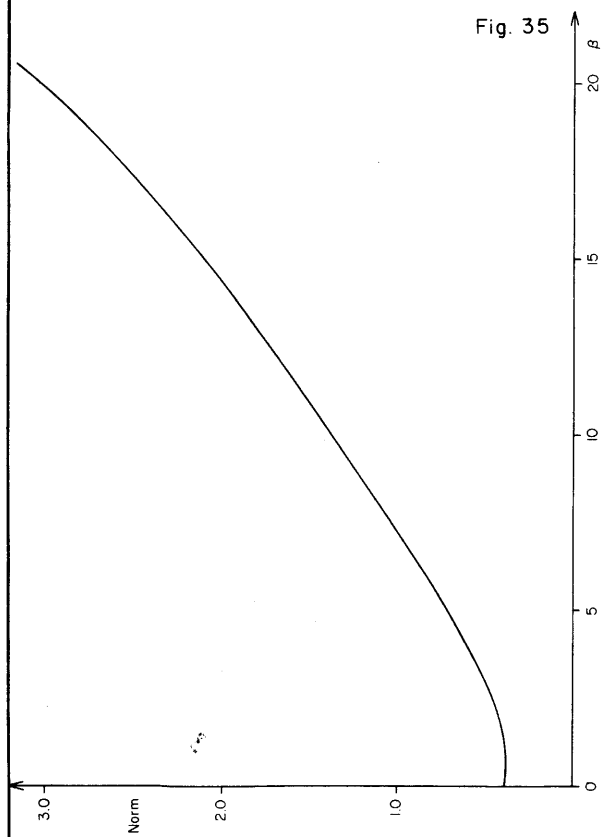

ORKUSTOFNUN

SIGALDA
Linear flow component β
vs. catchment loss / measured loss

80.07.29
SPK / GSJ
B-332
F. 19831

Fig. 36

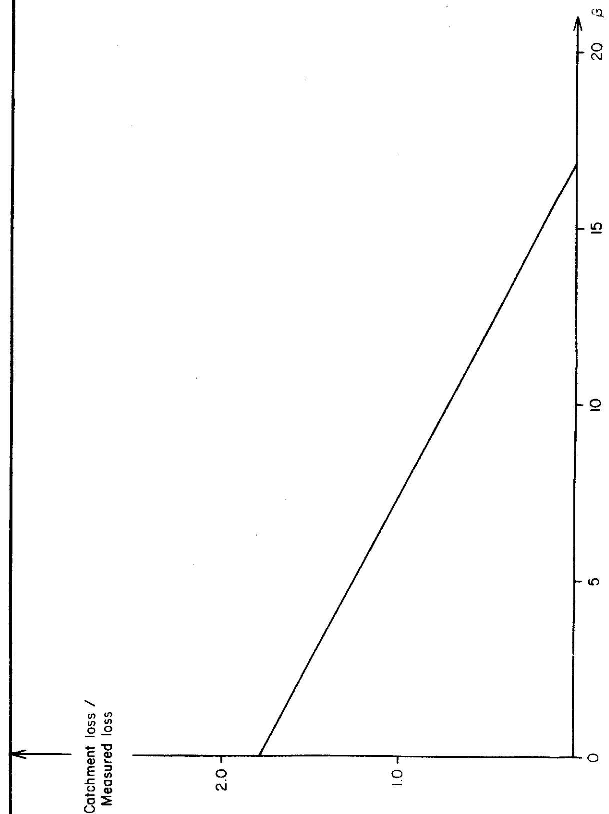

ORKUSTOFNUN
Jarðhitadeild

SIGALDA
Square flow component
Boundary flow parameter α vs. residual norm

80.07.29.
SPK / GSJ
B-332
F. 19834

Fig. 37

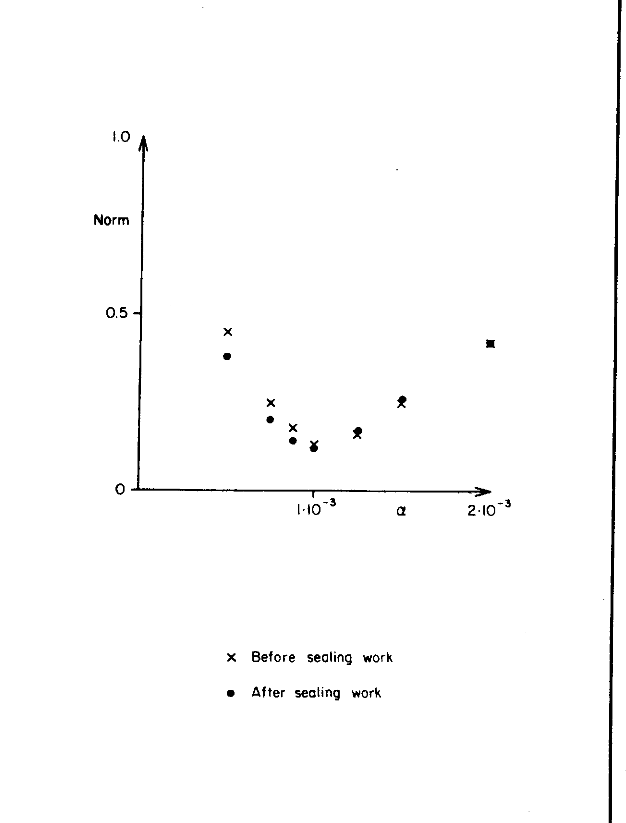

ORKUSTOFNUN

SIGALDA
Square flow component β
vs. residual norm

80.07.29.
SPK / GSJ
B-332
F. 19830

Fig. 38

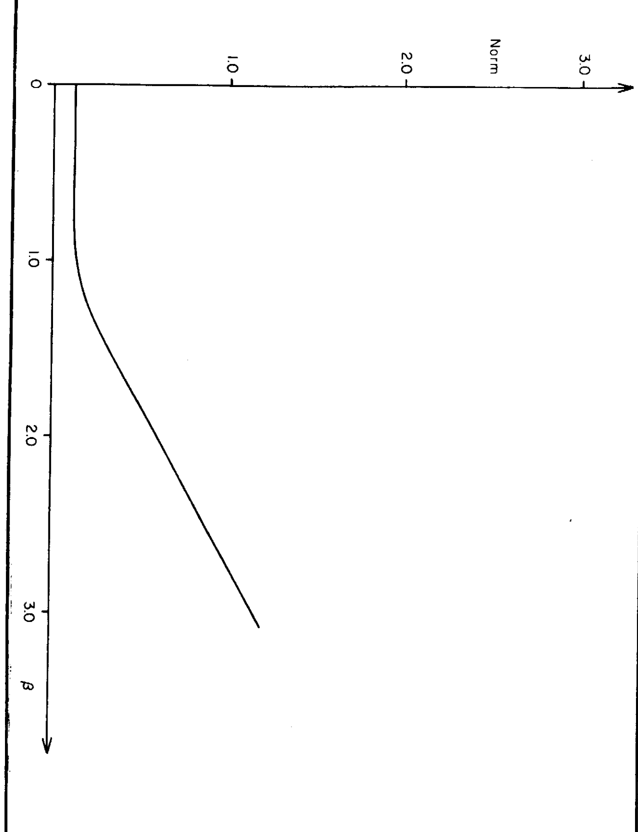

ORKUSTOFNUN
Jarðhitadeild

SIGALDA
Square flow component β vs.
Catchment loss/Measured loss

'80.09.01.
SPK / ÓD
B-332
F. 19949

Fig. 39

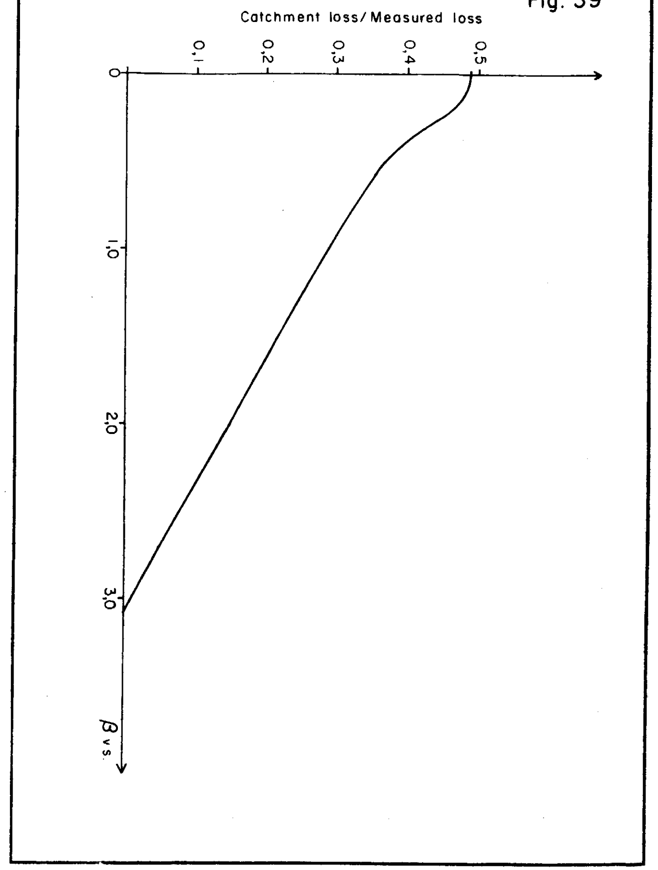

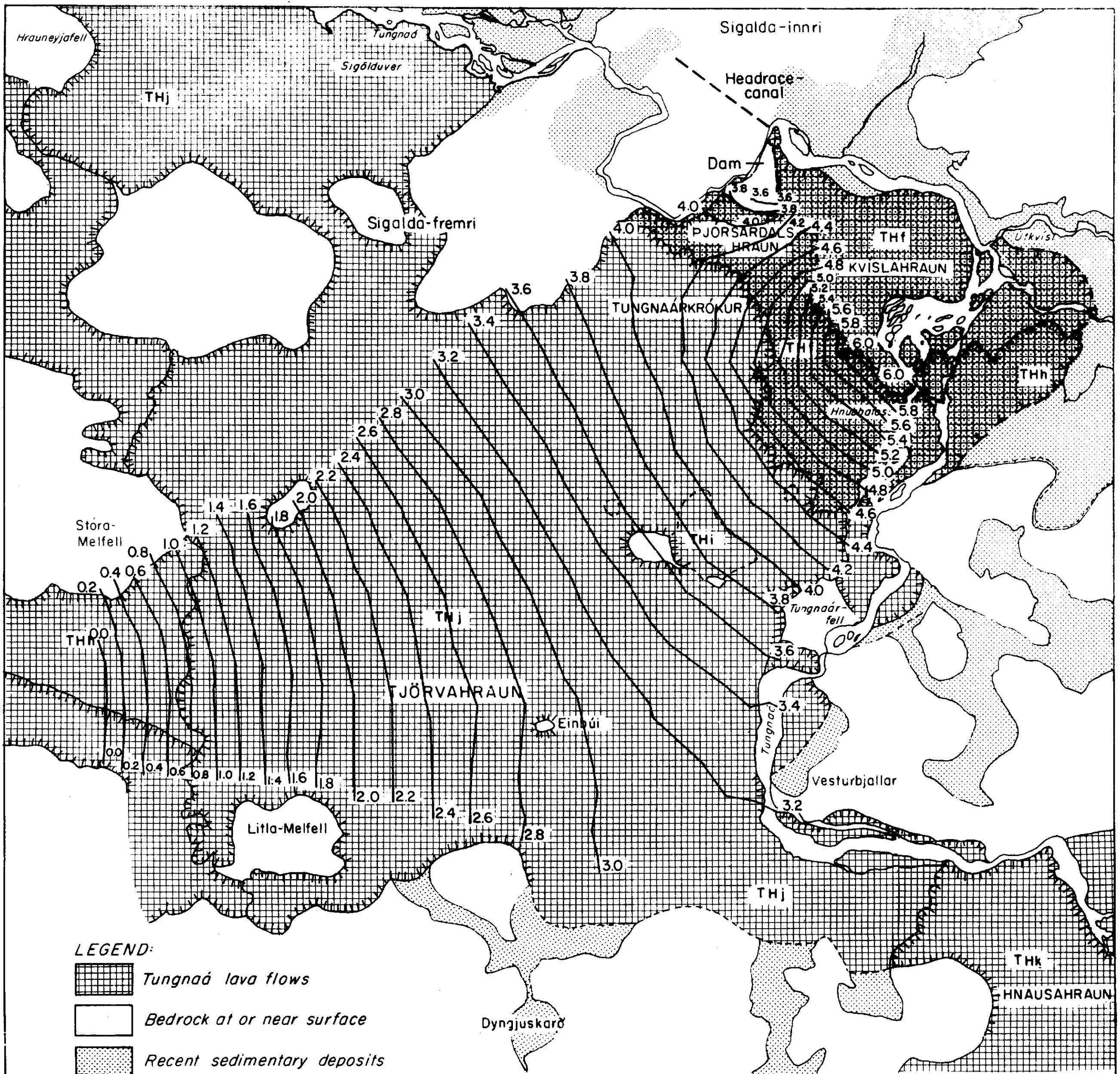

LEGEND:

- *Tungnaá lava flows*
- *Bedrock at or near surface*
- *Recent sedimentary deposits*
- *Sedimentary deposits on lava flows on Reservoir bottom.*
- *Lavafronts*
- *Equivalue lines for linear component pr. 10m reservoir level rise from linear flow zero level*

Fig. 40

SIGALDA

Linear component before sealing work
Model area

'80.09.01. SPK/ÓD B-332 F.19956

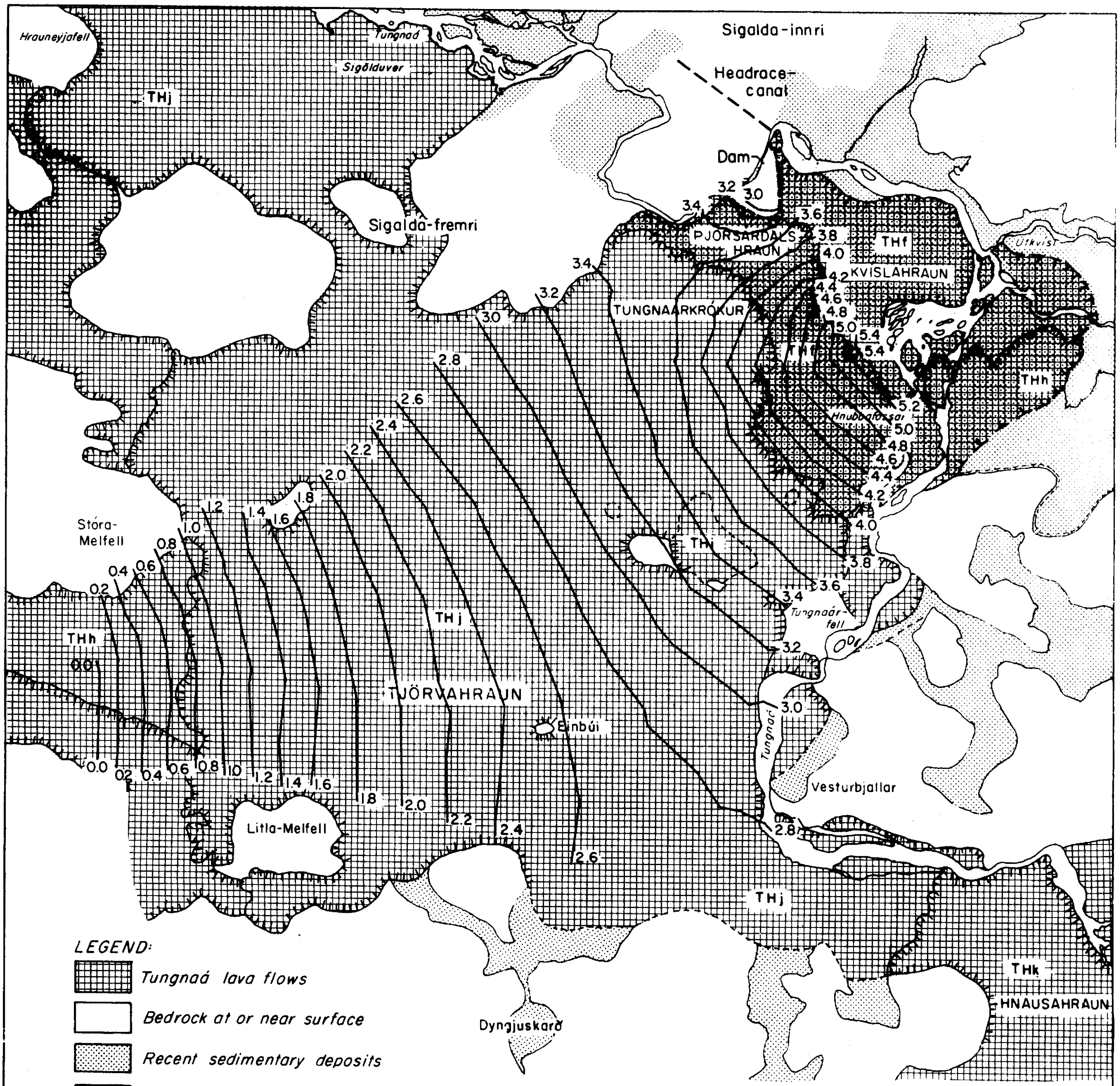

LEGEND:

- Tungnaá lava flows
- Bedrock at or near surface
- Recent sedimentary deposits
- Sedimentary deposits on lava flows on Reservoir bottom
- Lavafronts
- Equivalue lines for linear component pr. 10m reservoir level rise from linear flow zero level

Fig. 41

SIGALDA
Linear component after sealing work
Model area

'80.09.01. SPK/ÓD B-332 F. 19957

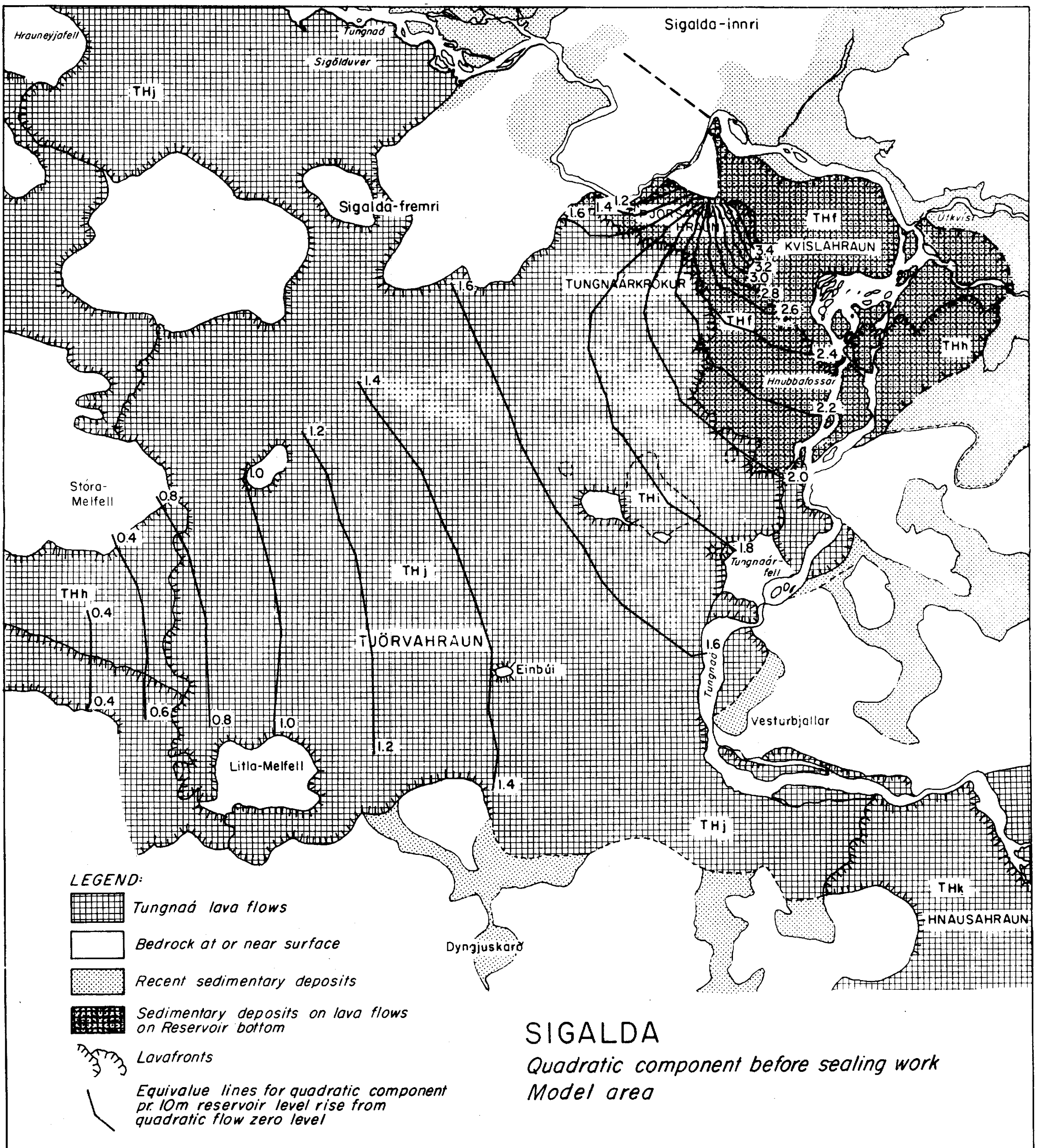

SIGALDA

Quadratic component before sealing work

Model area

Fig. 42

'80.09.01. SPK/ÓD B-332 F.19953

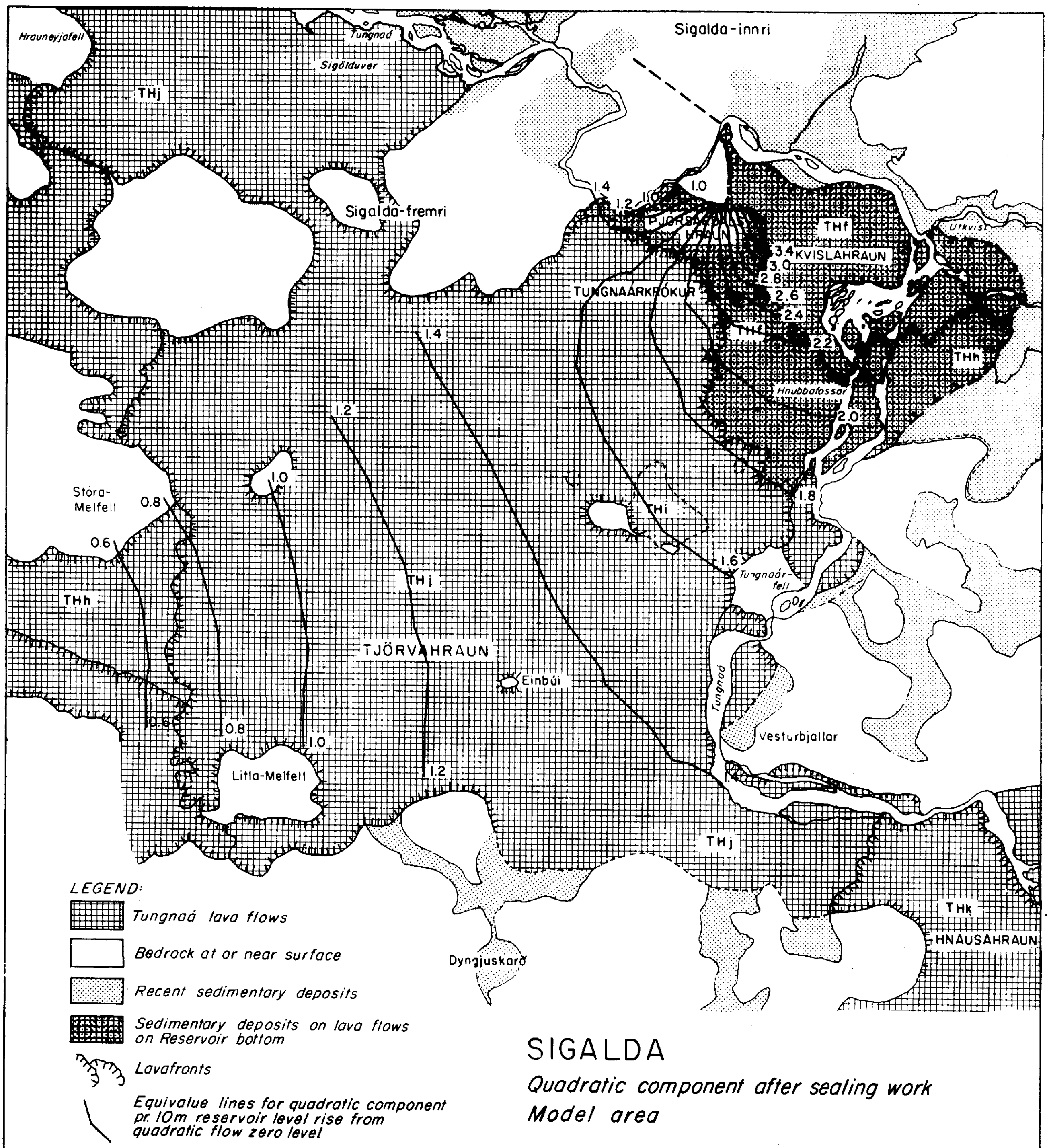

Fig. 43

SIGALDA

Quadratic component after sealing work

Model area

'80.09.01. SPK/ÓD B-332 F. 19954

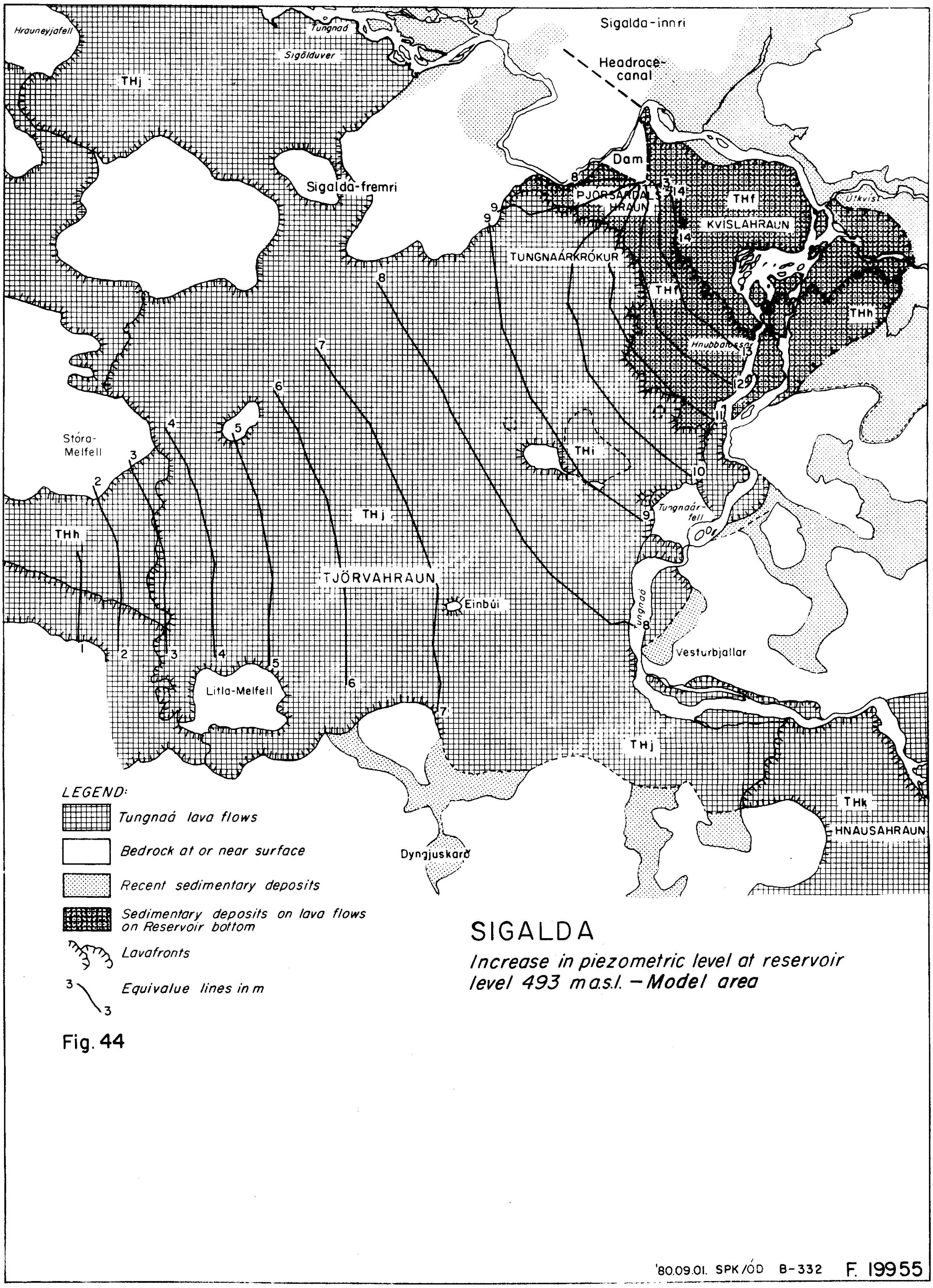

Fig. 44

SIGALDA

Increase in piezometric level at reservoir level 493 m.a.s.l. – Model area

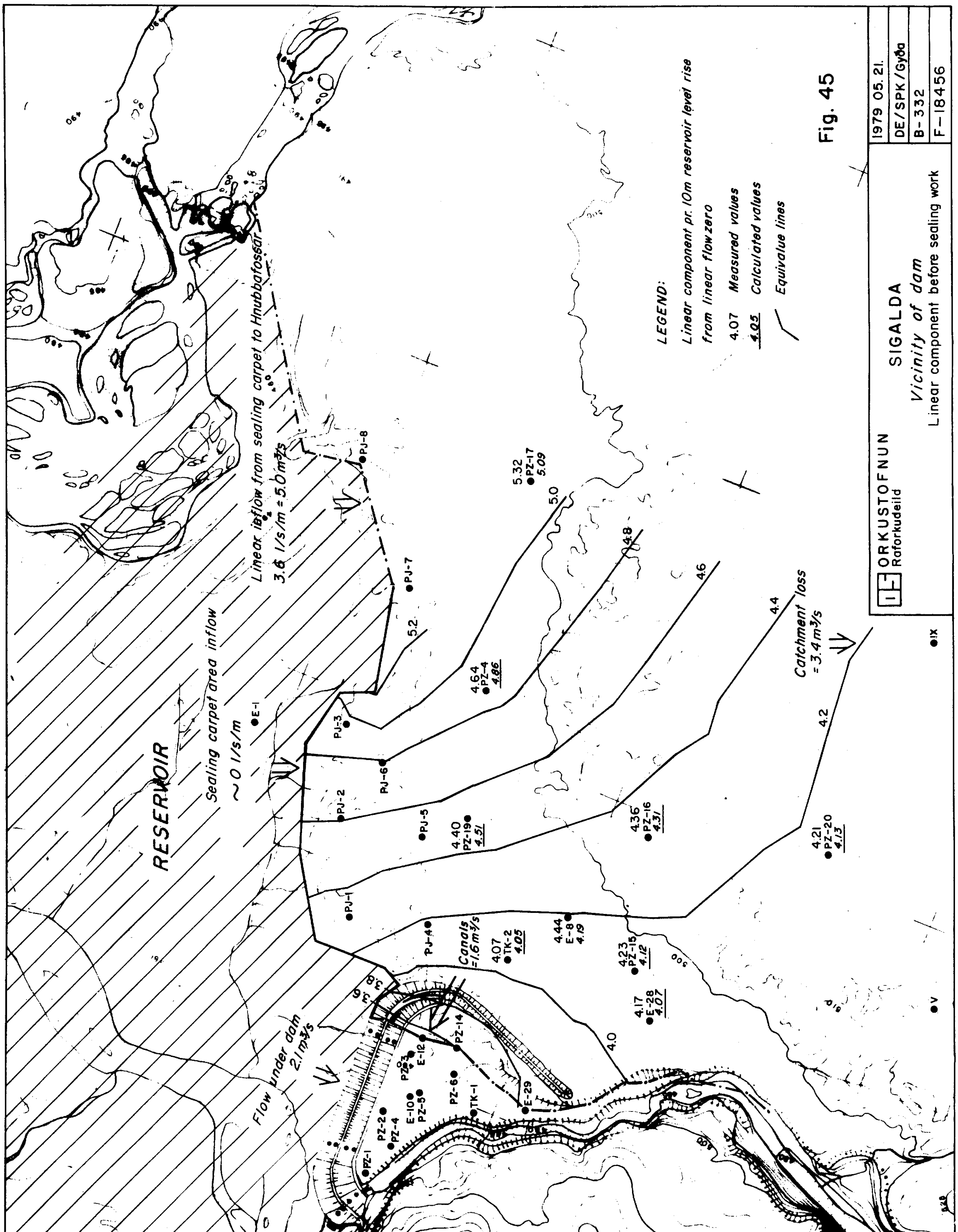
RESERVOIR
Sealing carpet area inflow
~0 l/s/m
Linear inflow from sealing carpet to Hnubbafossar
3.6 l/s/m = 5.0 m³/s
Flow under dam
2.1 m³/s
Canals
=1.6 m³/s
Catchment loss
=3.4 m³/s
5.2
5.0
4.8
4.6
4.4
4.2
4.0
5.32 PZ-17 5.09
4.64 PZ-4 4.86
4.40 PZ-19 4.51
4.36 PZ-16 4.31
4.21 PZ-20 4.13
4.07 TK-2 4.05
4.44 E-8 4.19
4.23 PZ-15 4.12
4.17 E-28 4.07
PJ-1
PJ-2
PJ-3
PJ-4
PJ-5
PJ-6
PJ-7
PJ-8
E-1
E-10
E-12
E-15
E-29
PZ-1
PZ-2
PZ-3
PZ-4
PZ-5
PZ-6
PZ-14
TK-1
IX
V
LEGEND:
Linear component pr. 10m reservoir level rise from linear flow zero
4.07 Measured values
4.05 Calculated values
Equivalue lines
Fig. 45
ORKUSTOFNUN
Raforkudeild
SIGALDA
Vicinity of dam
Linear component before sealing work
1979 05. 21.
DE/SPK/Gyða
B-332
F-18456

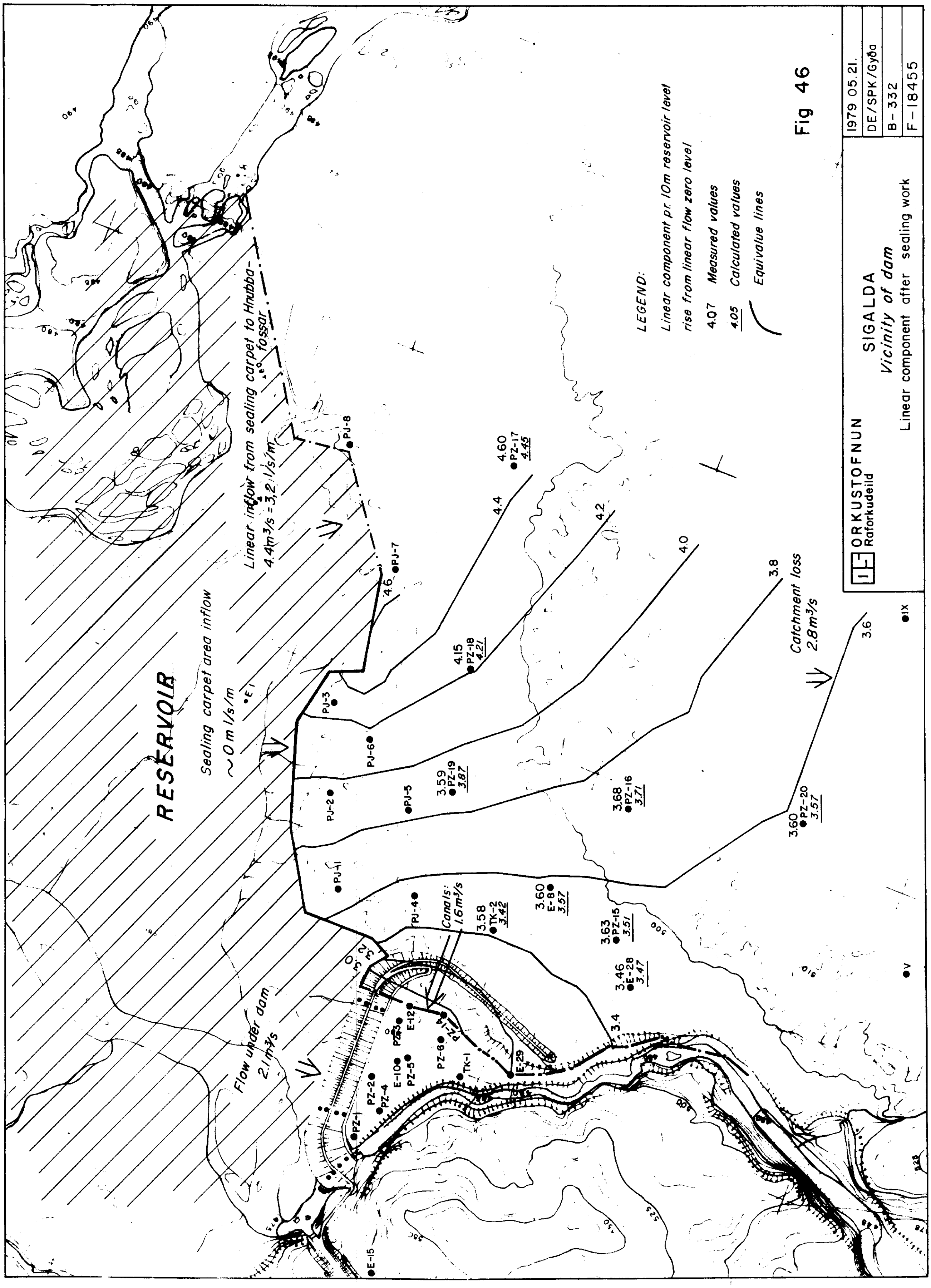
RESERVOIR
Sealing carpet area inflow
~0 m l/s/m
Linear inflow from sealing carpet to Hnubba-fossar
4.4m³/s = 3,2 l/s/m
Flow under dam
2.1 m³/s
Canals:
1.6 m³/s
Catchment loss
2.8 m³/s
4.6
4.4
4.2
4.0
3.8
3.6
3.4
4.60 PZ-17 4.45
4.15 PZ-18 4.21
3.59 PZ-19 3.87
3.68 PZ-16 3.71
3.60 PZ-20 3.57
3.60 E-8 3.57
3.58 TK-2 3.42
3.63 PZ-15 3.51
3.46 E-28 3.47
PJ-1
PJ-2
PJ-3
PJ-4
PJ-5
PJ-6
PJ-7
PJ-8
PZ-1
PZ-2
PZ-4
PZ-3
PZ-5
PZ-6
E-10
E-12
E-15
E-29
TK-1
E 1
IX
V
LEGEND:
Linear component pr. 10m reservoir level rise from linear flow zero level
4.07 Measured values
4.05 Calculated values
Equivalue lines
Fig 46
ORKUSTOFNUN
Raforkudeild
SIGALDA
Vicinity of dam
Linear component after sealing work
1979 05.21.
DE/SPK/Gyða
B-332
F-18455

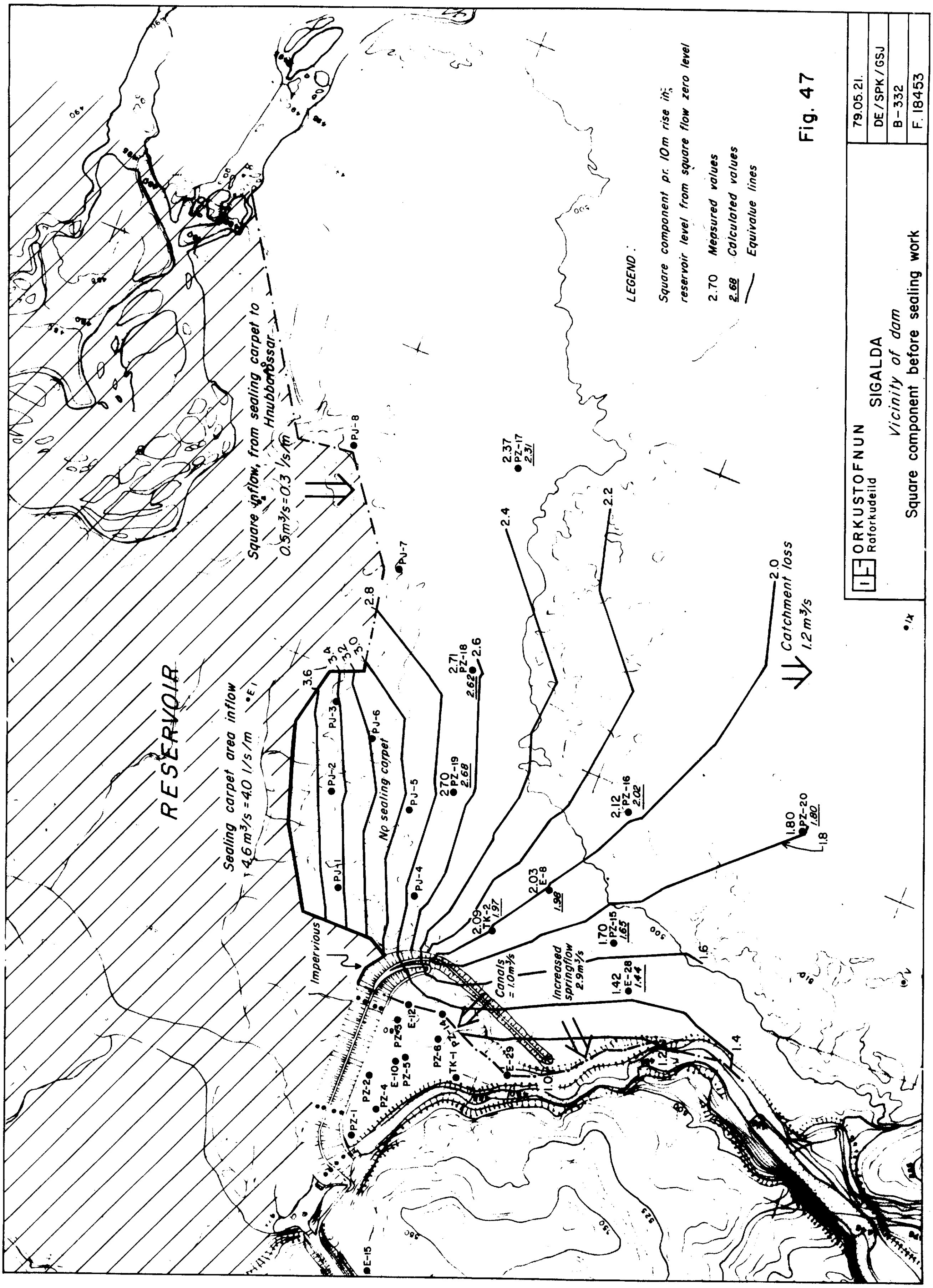
RESERVOIR
Sealing carpet area inflow
4.6 m³/s = 4.0 l/s/m
Square inflow, from sealing carpet to Hnubbafossar
0.5 m³/s = 0.3 l/s/m
No sealing carpet
Impervious
Canals = 1.0 m³/s
Increased springflow 2.9 m³/s
Catchment loss
1.2 m³/s
LEGEND:
Square component pr. 10m rise in reservoir level from square flow zero level
2.70 Measured values
2.68 Calculated values
Equivalue lines
ORKUSTOFNUN
Raforkudeild
SIGALDA
Vicinity of dam
Square component before sealing work
79.05.21.
DE/SPK/GSJ
B-332
F. 18453
Fig. 47

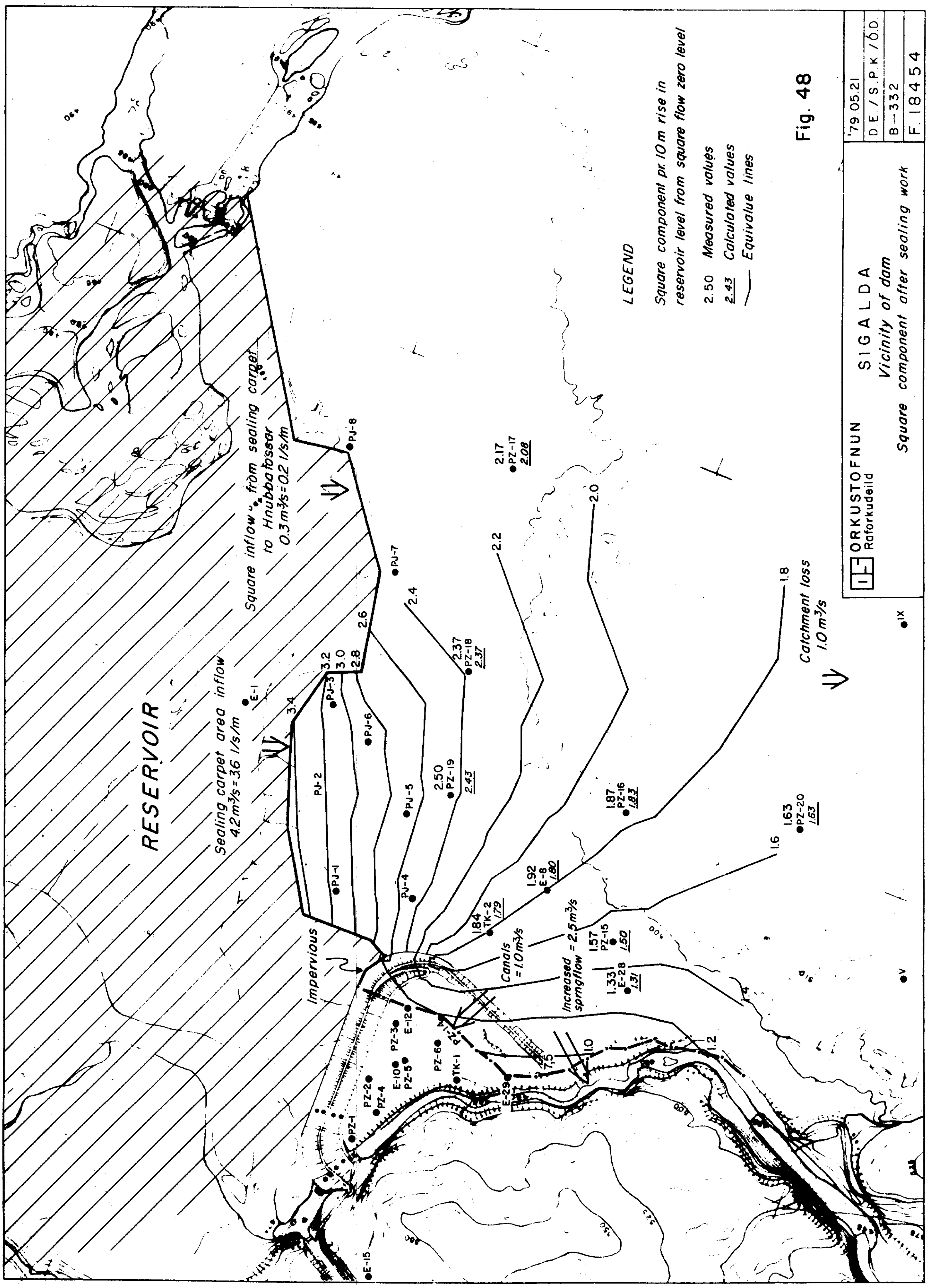
RESERVOIR
Sealing carpet area inflow
4.2 m³/s = 3.6 l/s/m
Square inflow from sealing carpet
to Hnubbafossar
0.3 m³/s = 0.2 l/s/m
Impervious
Canals
= 1.0 m³/s
Increased
springflow = 2.5 m³/s
Catchment loss
1.0 m³/s
LEGEND
Square component pr. 10 m rise in
reservoir level from square flow zero level
2.50 Measured values
2.43 Calculated values
Equivalue lines
ORKUSTOFNUN
Raforkudeild
SIGALDA
Vicinity of dam
Square component after sealing work
'79.05.21
D.E./S.P.K/Ó.D.
B-332
F. 18454
PJ-1
PJ-2
PJ-3
PJ-4
PJ-5
PJ-6
PJ-7
PJ-8
E-1
2.50 PZ-19 2.43
2.37 PZ-18 2.37
2.17 PZ-17 2.08
1.87 PZ-16 1.83
1.63 PZ-20 1.63
1.92 E-8 1.80
1.84 TK-2 1.79
1.57 PZ-15 1.50
1.33 E-28 1.31
3.4
3.2
3.0
2.8
2.6
2.4
2.2
2.0
1.8
1.6
1.2
1.0
PZ-1
PZ-2
PZ-3
PZ-4
PZ-5
PZ-6
E-10
E-12
E-15
E-29
TK-1
Fig. 48

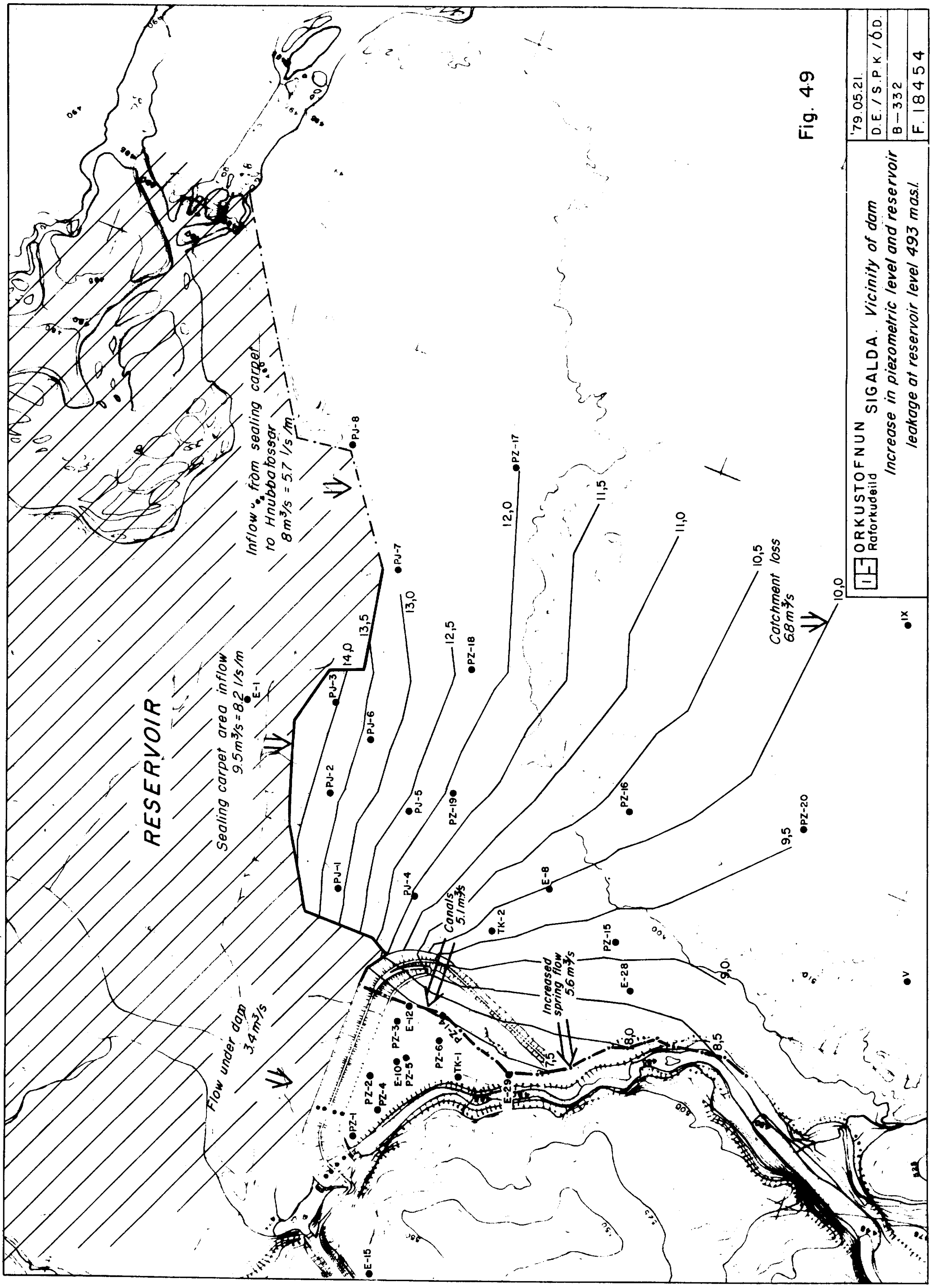
RESERVOIR
Sealing carpet area inflow
9.5 m³/s = 8.2 l/s/m
Inflow from sealing carpet
to Hnubbafossar
8 m³/s = 5.7 l/s/m
Flow under dam
3.4 m³/s
Canals
5.1 m³/s
Increased
spring flow
5.6 m³/s
Catchment loss
6.8 m³/s
14,0
13,5
13,0
12,5
12,0
11,5
11,0
10,5
10,0
9,5
9,0
8,5
8,0
7,5
PJ-1
PJ-2
PJ-3
PJ-4
PJ-5
PJ-6
PJ-7
PJ-8
PZ-1
PZ-2
PZ-3
PZ-4
PZ-5
PZ-6
PZ-15
PZ-16
PZ-17
PZ-18
PZ-19
PZ-20
E-1
E-8
E-10
E-12
E-15
E-28
E-29
TK-1
TK-2
IX
V
ORKUSTOFNUN
Raforkudeild
SIGALDA. Vicinity of dam
Increase in piezometric level and reservoir
leakage at reservoir level 493 m.a.s.l.
'79.05.21.
D.E./S.P.K./Ó.D.
B-332
F. 18454

Fig. 49

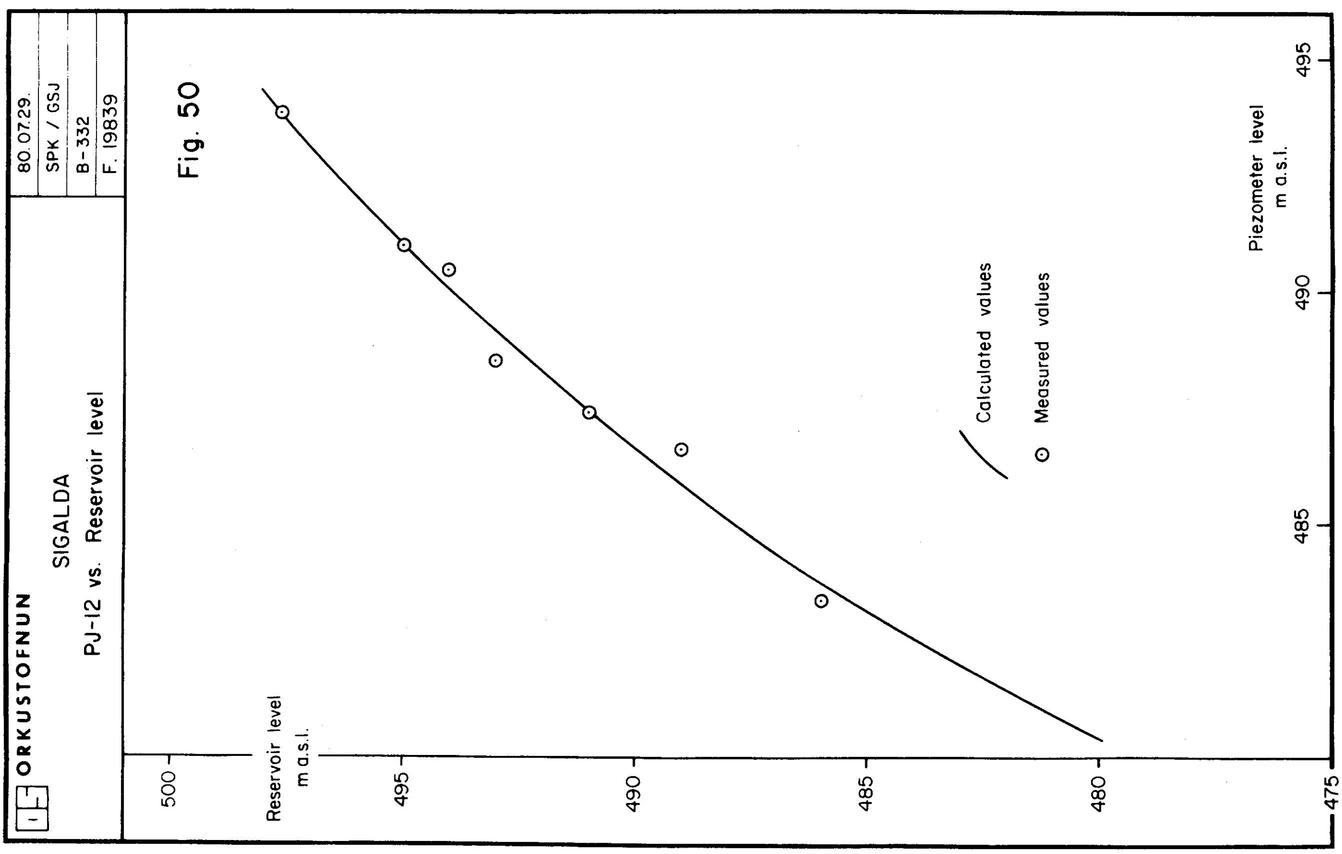
ORKUSTOFNUN
SIGALDA
PJ-12 vs. Reservoir level
80.07.29.
SPK / GSJ
B-332
F. 19839
Calculated values
Measured values
Reservoir level
m a.s.l.
Piezometer level
m a.s.l.
500
495
490
485
480
475
495
490
485

Fig. 50

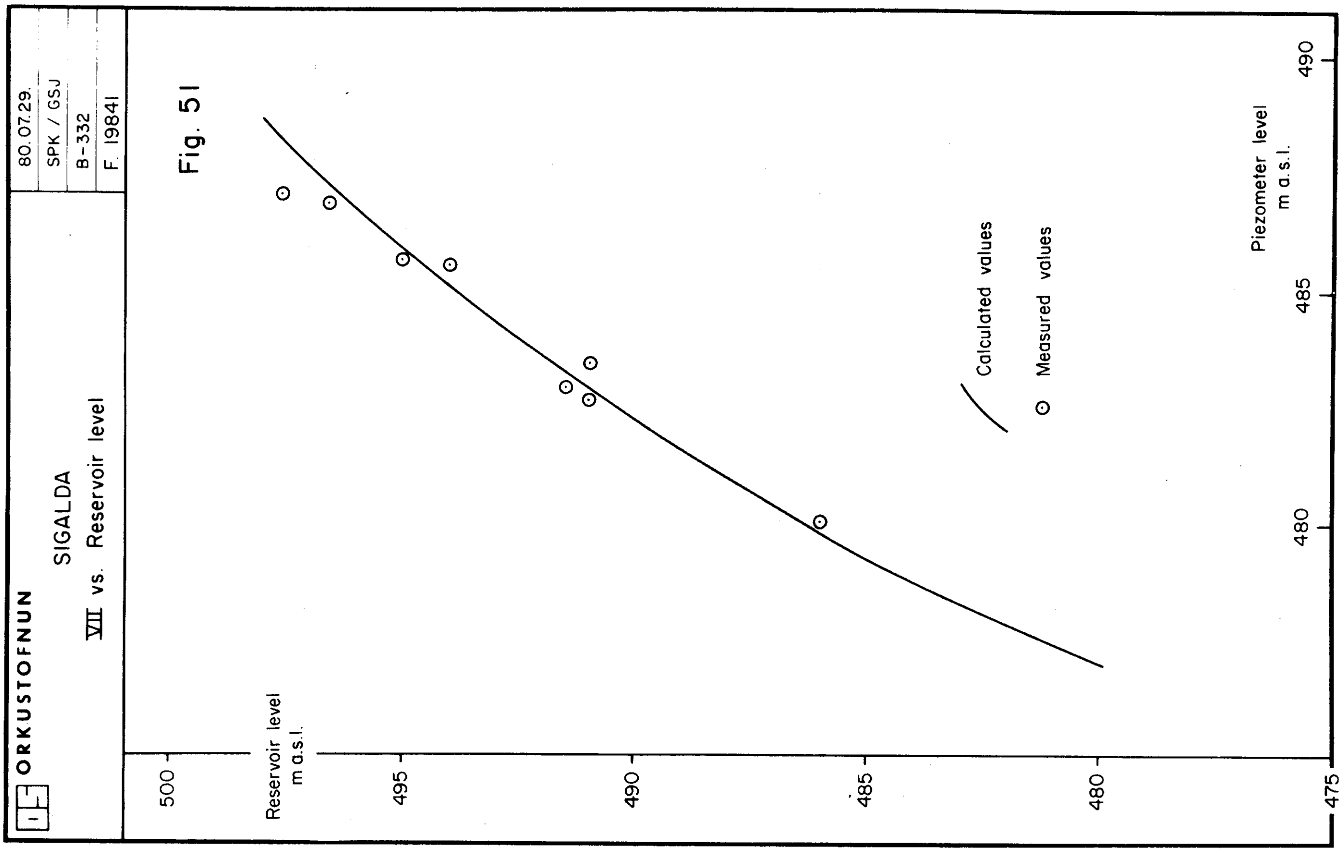
ORKUSTOFNUN
SIGALDA
VII vs. Reservoir level
80.07.29.
SPK / GSJ
B-332
F. 19841
Calculated values
Measured values
Reservoir level
m a.s.l.
Piezometer level
m a.s.l.
500
495
490
485
480
475
490
485
480

Fig. 51

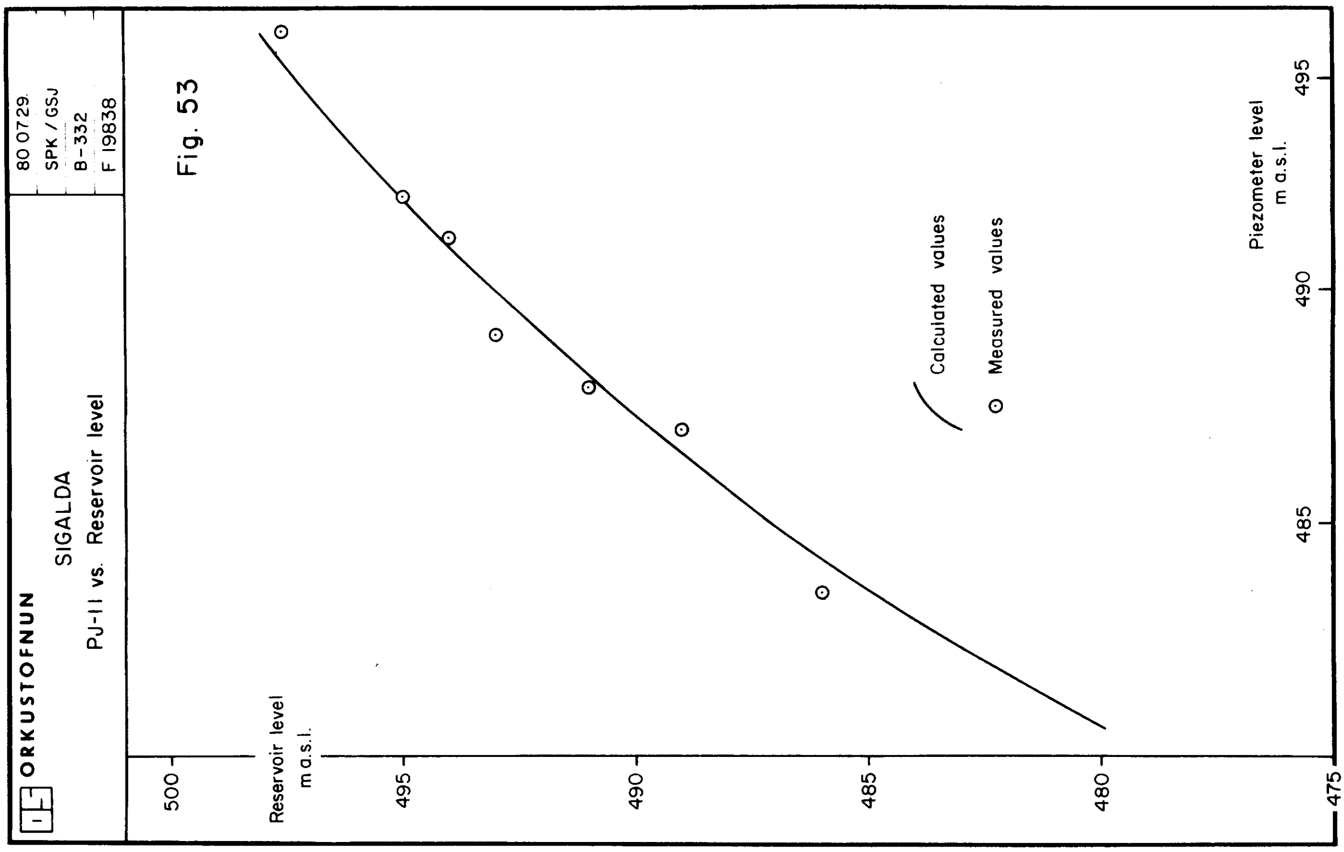
ORKUSTOFNUN
SIGALDA
PJ-11 vs. Reservoir level
80 07 29.
SPK / GSJ
B-332
F 19838
Reservoir level
m a.s.l.
500
495
490
485
480
475
Piezometer level
m a.s.l.
485
490
495
Calculated values
Measured values

Fig. 53

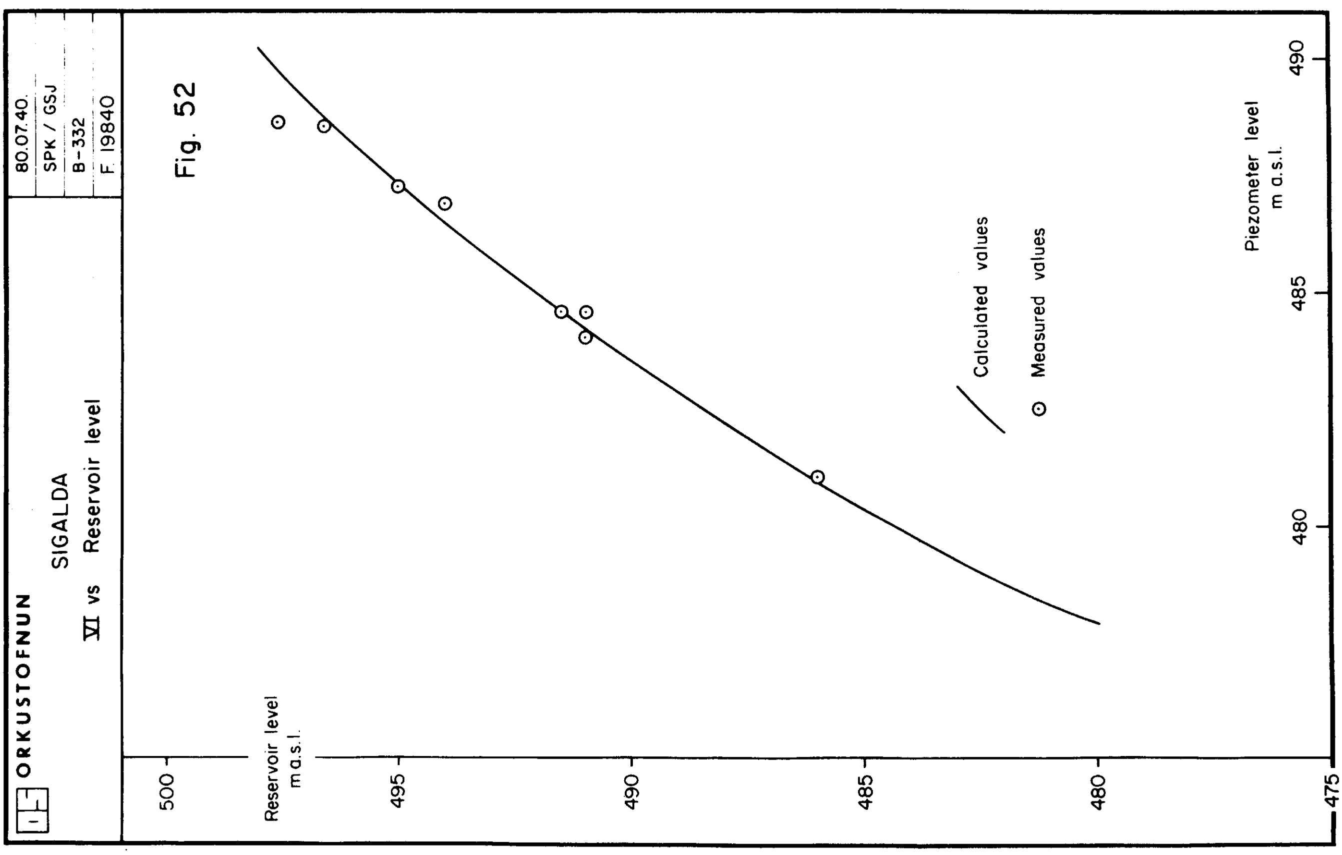
ORKUSTOFNUN
SIGALDA
VI vs Reservoir level
80.07.40.
SPK / GSJ
B-332
F 19840
Reservoir level
m a.s.l.
500
495
490
485
480
475
Piezometer level
m a.s.l.
480
485
490
Calculated values
Measured values

Fig. 52

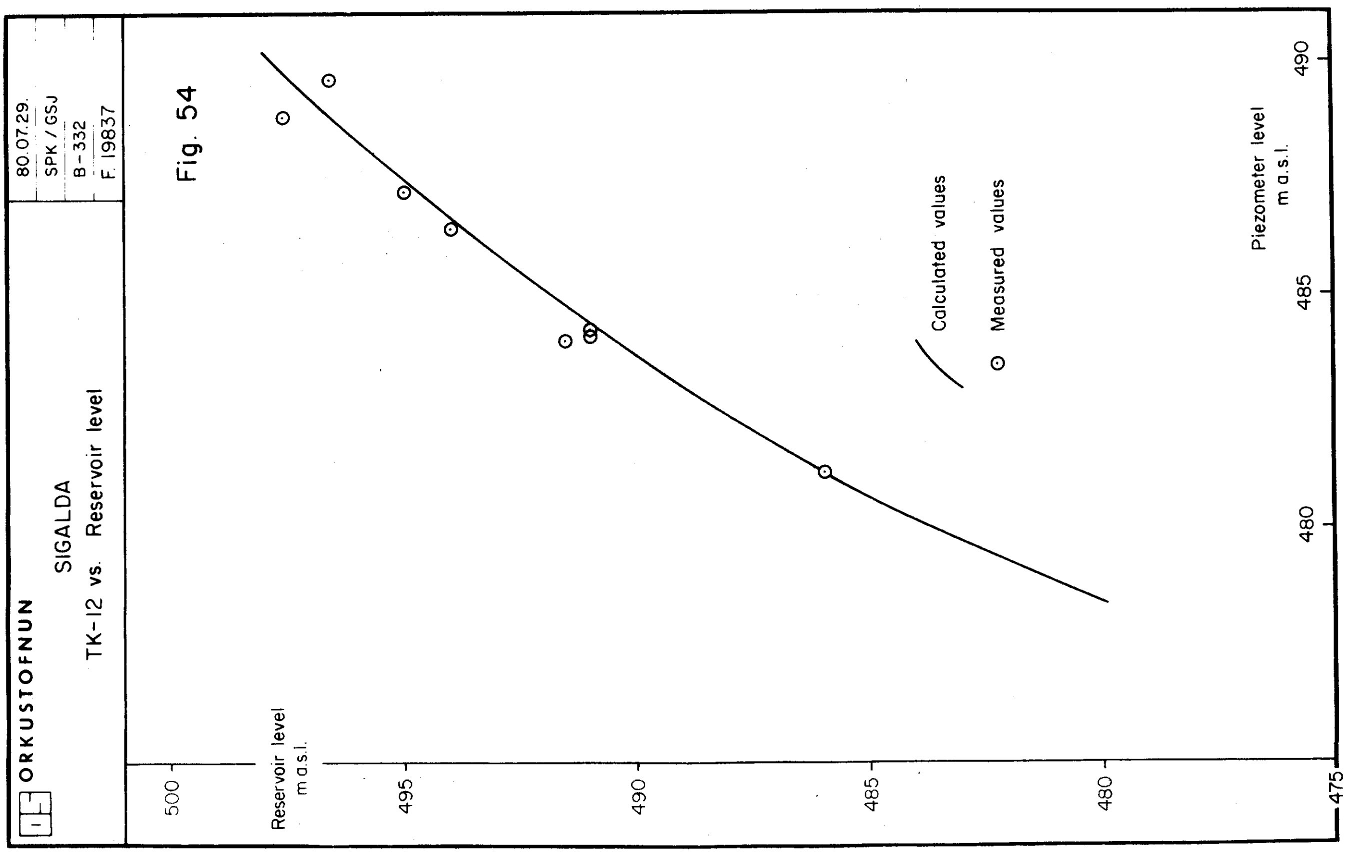
ORKUSTOFNUN
SIGALDA
TK-12 vs. Reservoir level
80.07.29.
SPK / GSJ
B-332
F. 19837
Calculated values
Measured values
Reservoir level
m a.s.l.
Piezometer level
m a.s.l.
500
495
490
485
480
475
490
485
480

Fig. 54

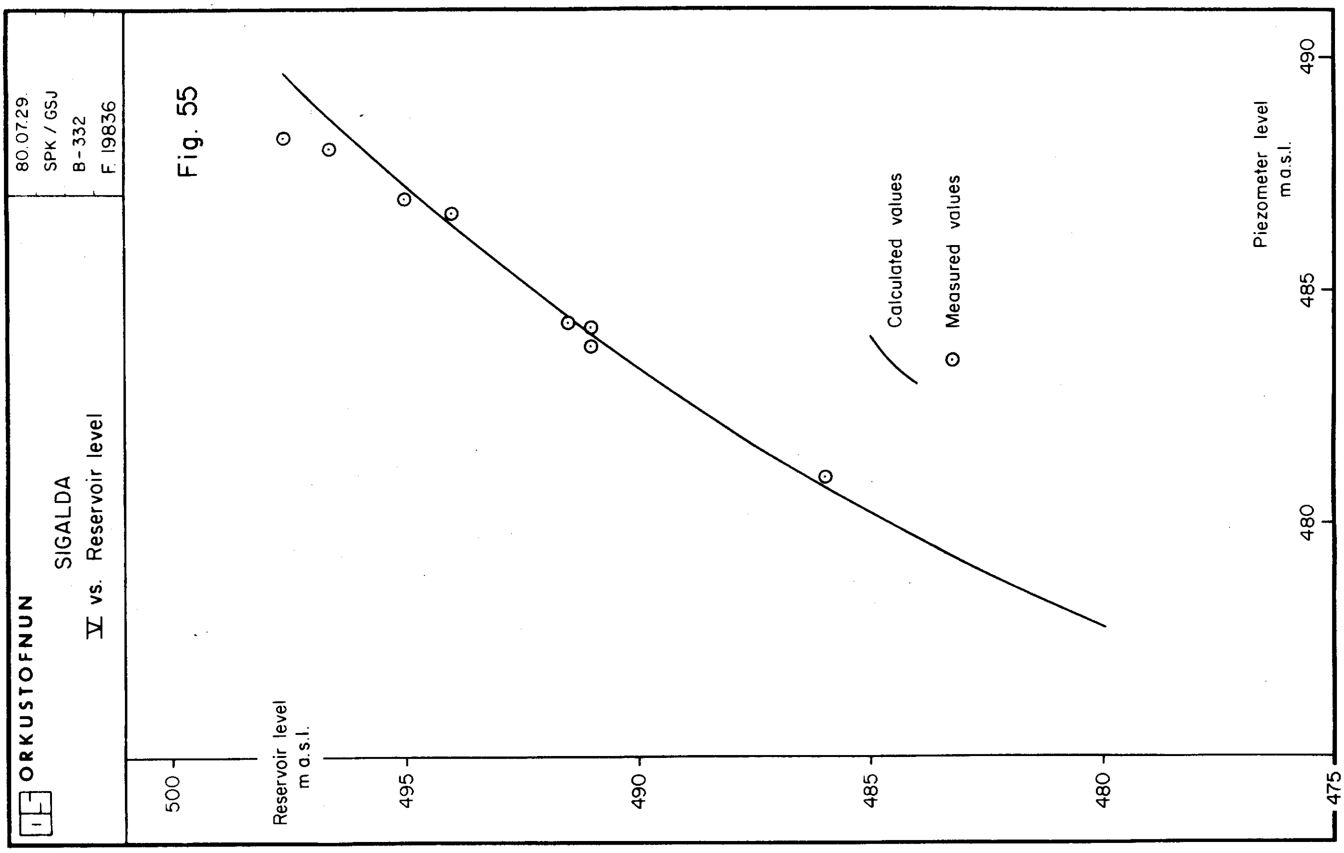
ORKUSTOFNUN
SIGALDA
V vs. Reservoir level
80.07.29.
SPK / GSJ
B-332
F. 19836
Calculated values
Measured values
Reservoir level
m a.s.l.
Piezometer level
m a.s.l.
500
495
490
485
480
475
490
485
480

Fig. 55

'80.09.01. SPK/ÓD
B-332
F. 19951

SIGALDA
IX vs. Reservoir level

Fig. 56

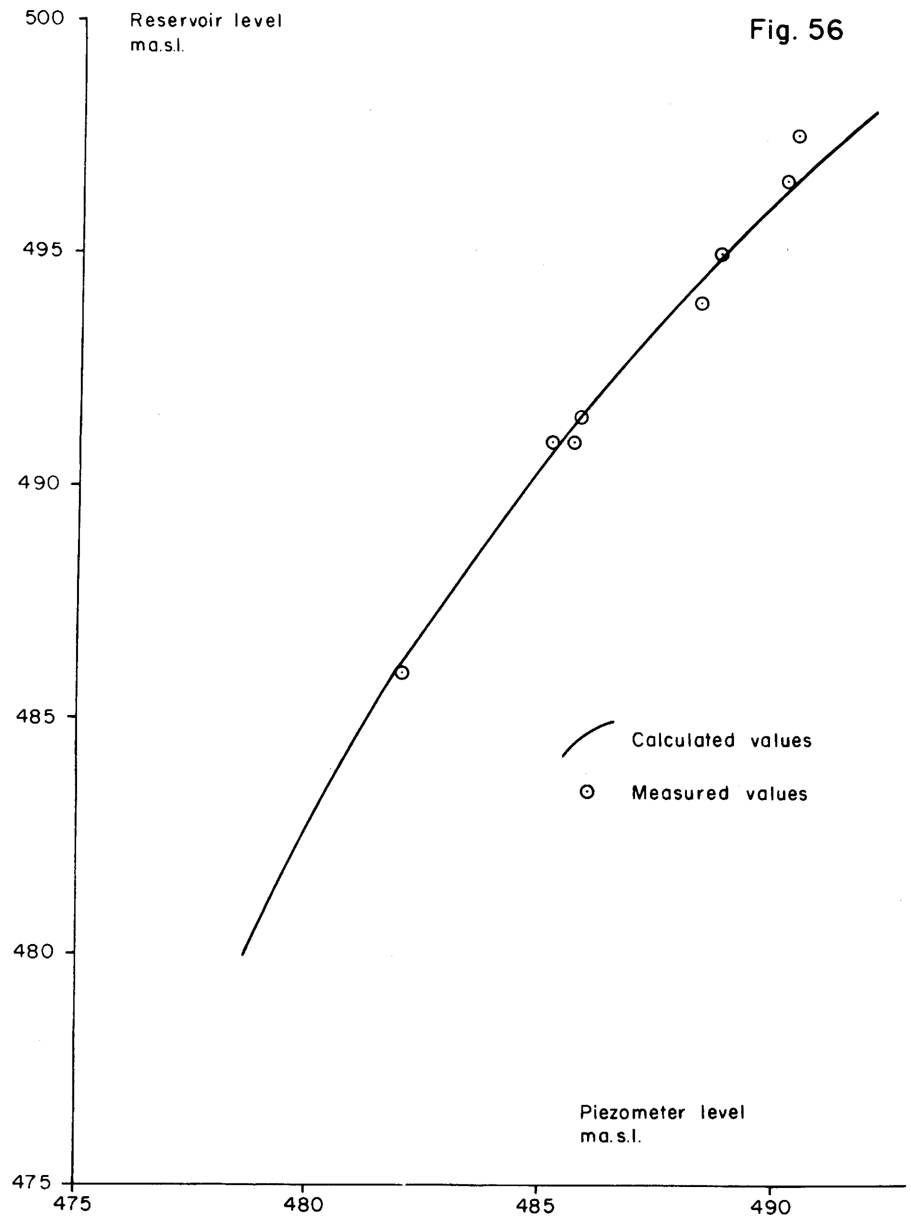

ORKUSTOFNUN
Jarðhitadeild

SIGALDA
Maximum effect of sealing carpet
vs. reservoir level

80.07.29.
SPK / GSJ
B-332
F. 19835

Fig. 57

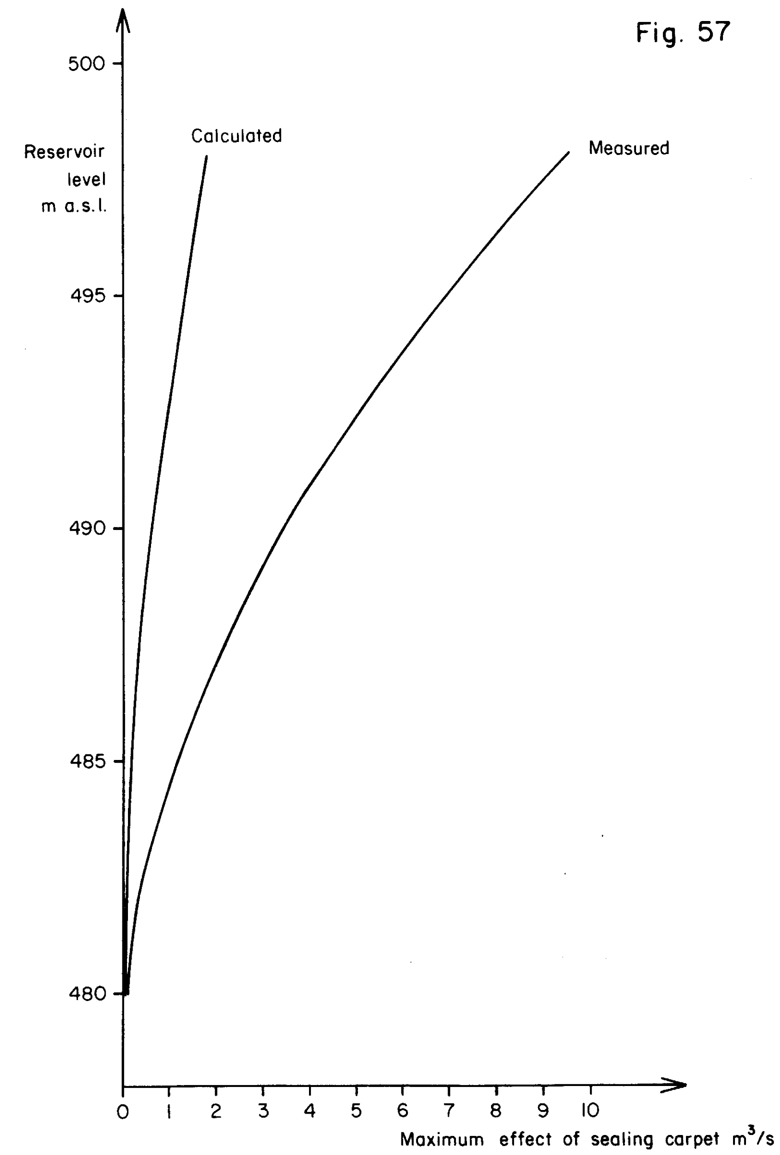

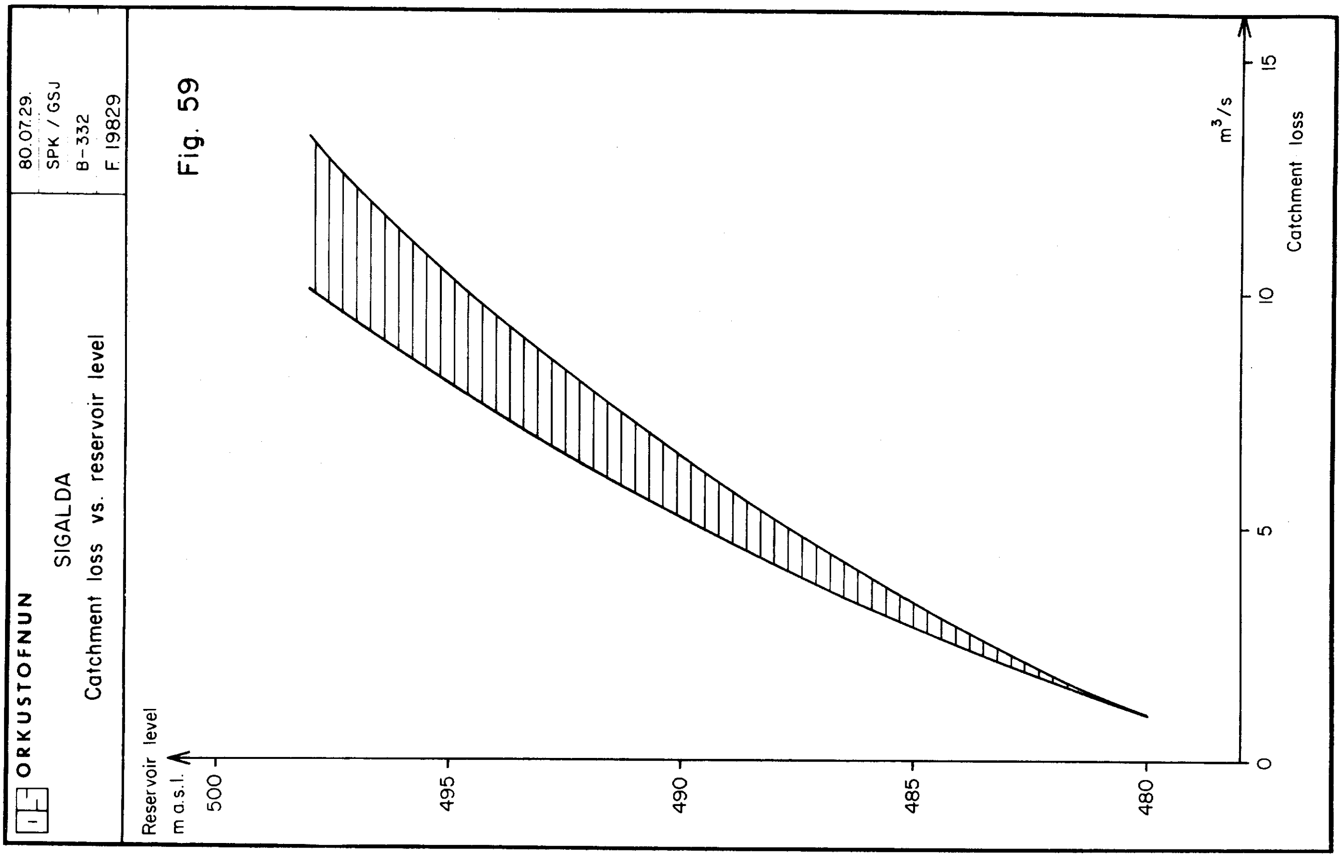
ORKUSTOFNUN
SIGALDA
Catchment loss vs. reservoir level
80.07.29.
SPK / GSJ
B-332
F. 19829
Reservoir level
m a.s.l.
500
495
490
485
480
0
5
10
15
m³/s
Catchment loss
Fig. 59

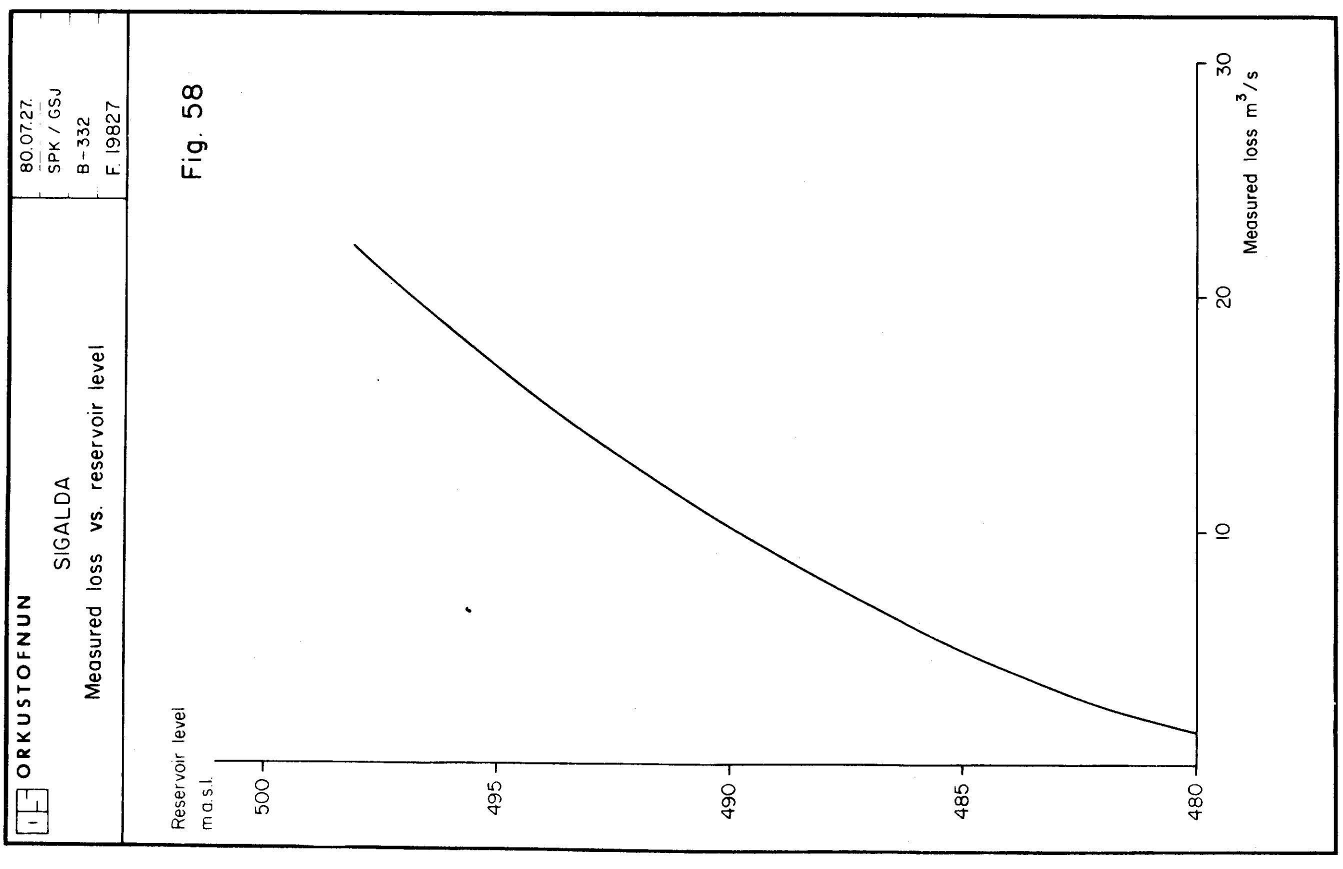
ORKUSTOFNUN
SIGALDA
Measured loss vs. reservoir level
80.07.27.
SPK / GSJ
B-332
F. 19827
Reservoir level
m a.s.l.
500
495
490
485
480
10
20
30
Measured loss m³/s
Fig. 58

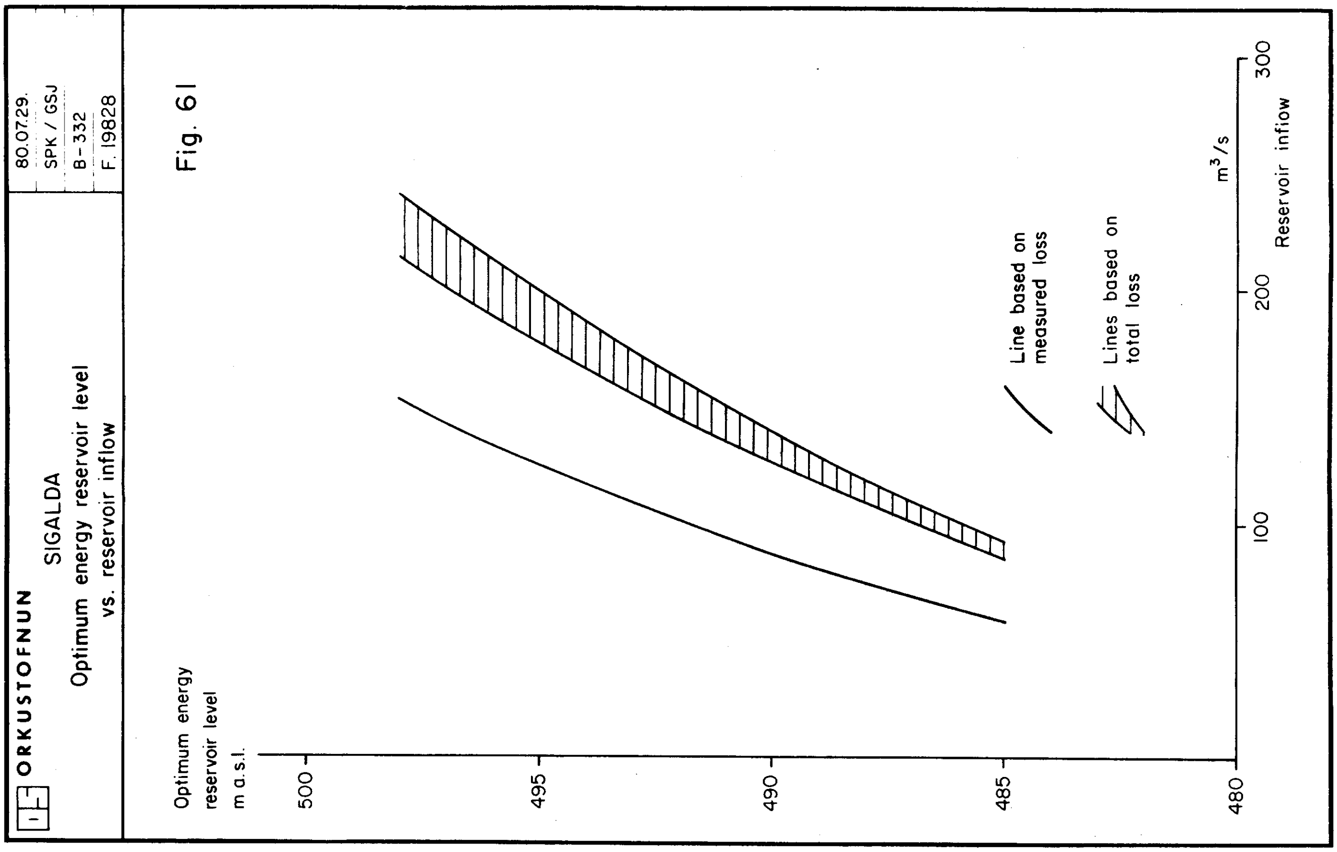
ORKUSTOFNUN
SIGALDA
Optimum energy reservoir level
vs. reservoir inflow
80.07.29.
SPK / GSJ
B-332
F. 19828
Fig. 61
Optimum energy
reservoir level
m a.s.l.
500
495
490
485
480
100
200
300
m³/s
Reservoir inflow
Line based on
measured loss
Lines based on
total loss

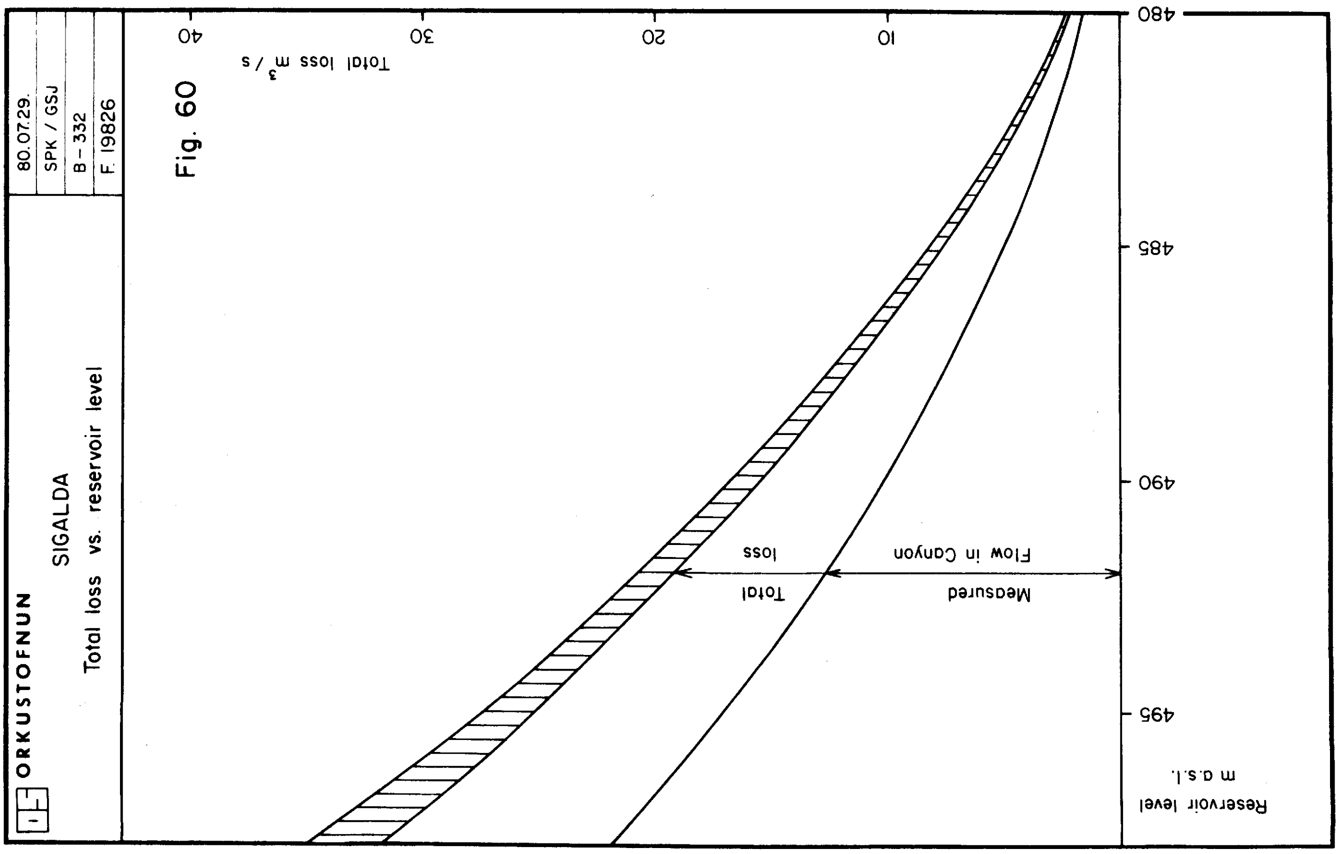
ORKUSTOFNUN
SIGALDA
Total loss vs. reservoir level
80.07.29.
SPK / GSJ
B-332
F. 19826
Fig. 60
40
30
20
10
Total loss m³/s
Reservoir level
m a.s.l.
495
490
485
480
Total
loss
Measured
Flow in Canyon